Aeolian Research 77 (2026) 101063

Contents lists available at ScienceDirect

Aeolian Research

journal homepage: www.elsevier.com/locate/aeolia

Suspended aeolian sand transport across a remobilized coastal dune system, Zuid-Kennemerland, The Netherlands

O. Verhage [a,c,*], S.M. Arens [b], C.J. Beets [a], J.B.W. Stuut [a,c], G. van Zijl [d], M.A. Prins [a]

[a] Earth Sciences Department, Vrije Universiteit Amsterdam, The Netherlands
[b] Arens Bureau voor Strand-en Duinonderzoek, The Netherlands
[c] Ocean Systems Department, NIOZ, The Netherlands
[d] Provinciaal Waterleidingbedrijf Noord-Holland (PWN), The Netherlands

ARTICLE INFO

Keywords:
Foredune notch
Reactivated parabolic dune
Suspended aeolian transport
Sand trap
Dune morphodynamics

ABSTRACT

Coastal dunes are important features of sandy coasts due to their multifunctionality. In recent decades, dune management has shifted from *stabilization* towards *remobilization* to enhance coastal resilience and biodiversity. This study investigates a remobilized dune system in Zuid-Kennemerland, along the Dutch west coast, where multiple artificial foredune notches and reactivated parabolic dunes (RPD's) were created in 2013. Over more than a decade, 15 sand traps monitored suspended aeolian sand transport, with samples correlated to meteorological data and geomorphological changes. Up to 89% of annual suspended sand load occurs during storm events (with average hourly wind speeds >20.8 m/s) with sand deposition reaching 1200 m inland of the foredune. Sand traps downwind of notches indicate declining suspended loads over time because flow acceleration and sedimentation declines as notches become wider. In contrast, traps downwind of RPD's indicate increasing suspended sand transport, related to the landward migration of depositional lobes. In unnotched areas, continuous suspended load trends align with the general linear growth of Dutch foredunes. Volumetric analyses indicate that notches and blowouts have created a transport corridor connecting the beach and hinterland. These findings emphasize the significance of suspended aeolian sand transport in accounting for spatial variation in reactivated dune systems. The results also contribute to improved morphodynamic coastal models since the importance of suspended transport has to date been underrecognized. Future research should quantify depositional patterns and sediment characteristics to clarify their roles in dune evolution, soil formation, and ecosystem development.

1. Introduction

The sandy coastal zone is increasingly under pressure from rising sea levels and anthropogenic activities, leading to significant decline of this vital landscape (Hallin et al., 2019; Lansu et al., 2024; Nawarat et al., 2024). Vegetation cover and topography exert an important control on erosion and deposition of sand, affecting sand transport patterns (Arens, 1996; Hesp, 2002; Walker and Hesp, 2013) and physical characteristics of the transported sand particles (Van Hateren et al., 2020). These processes shape diverse geomorphological features that support rich biodiversity. In the Netherlands, as in many other places around the world, coastal dune systems play a multifunctional role. They serve as protection against the sea, contain large freshwater reserves, harbour a specific and unique ecosystem, and function as nature reserves and recreation areas (Arens et al., 2020; Bakker et al., 1981; Bird et al., 2020; Creer et al., 2020).

Since the second half of the nineteenth century coastal management in the Netherlands, focused on stabilizing dunes through the planting of *Marram grass* (*Ammophila arenaria/Calamagrostis arenaria*) and pine trees. Combined with large-scale foreshore-, beach-, and dune nourishments, this stabilization has led to the formation of a high and steep foredune, and a decrease in aeolian sand transport towards the hinterland (Arens and Wiersma, 1994; Arens et al., 2013a; Arens et al., 2020; Brand et al., 2022; Ruessink et al., 2018). These interventions have resulted in reduced accumulation (or burial) rates by grain fall, the suspended sediment fall-out due to gravitational settling, in the hinterland (Aggenbach et al., 2018; Arens et al., 2013b). The lack of aeolian dynamics, together with increased nitrogen deposition, has contributed

* Corresponding author at: Vrije Universiteit Amsterdam, VUO Building, Room 10.91, De Boelelaan 1100, 1081HZ Amsterdam, The Netherlands.
E-mail address: o.verhage@vu.nl (O. Verhage).

https://doi.org/10.1016/j.aeolia.2026.101063
Received 17 October 2025; Received in revised form 30 April 2026; Accepted 14 June 2026
1875-9637/© 2026 The Author(s). Published by Elsevier B.V. This is an open access article under the CC BY license (http://creativecommons.org/licenses/by/4.0/).

to an increase in grass encroachment and a decline in biodiversity (Kooijman and De Haan, 1995; Miyanishi and Johnson, 2021; Robin et al., 2023; Ruessink et al., 2018).

In response to these developments, the management of Dutch coastal dunes has shifted towards strategies aiming at improving ecology and protecting habitats and species (Kuipers and Van der Vegte, 2016; Ruessink et al., 2018; Van der Meulen and Jungerius, 1989). One of these strategies is dune remobilization by creating notches, reactivated parabolic dunes (RPD), and blowouts, focusing on the restoration of aeolian sand transport from the beach/foredune complex towards the hinterland (Arens et al., 2013a; De Jong et al., 2014; Meerkerk et al., 2007; Riksen et al., 2016; Ruessink et al., 2018). A total of 116 foredune trough blowouts and notches are present in the Dutch coastal dunes, of which 63 were created by human intervention. The creation of foredune notches to reactivate dune systems has gained popularity in multiple countries, especially the United Kingdom and the Netherlands (Ruessink et al., 2026; Pagon et al., 2025). Although there is a rise in popularity, the need for reactivated dune systems remains debated (Cooper and Jackson, 2021; Delgado-Fernandez et al., 2019).

Dune dynamics operate at different timescales: fast response (seconds/hourly/daily) and slow response processes (yearly/decadal). Fast response processes are related to wind gusts and storm events, while slow response processes are influenced by yearly longer-term meteorological conditions (e.g. windiness, tidal influences/storm surges and precipitation) (De Ruig, 1989). Storm events are a dominant factor in sandy beach and dune systems (Ciavola et al., 2015), both because of wave and wind erosion and sedimentation. Changing climate conditions can change the frequency of fast response processes, causing a change in slow response processes. Affecting the overall sand budget, the erosion and accretion of sand, the precipitation and moisture balance, groundwater composition, acidification or calcification of soils as well as the total vegetation cover and the composition and degradation of vegetation (Noest et al., 1995).

Previous research on aeolian transport has largely focused on saltation transport, while field experiments addressing modified saltation and suspension transport have received significantly less attention (Petersen et al., 2011; Van Hateren et al., 2020). However, ample evidence suggests that sand transported by modified saltation and suspension is an important process occurring in active dune forms (e.g. Anderson and Walker, 2006; Arens et al., 2002; Arens et al., 2012; Arens et al., 2013b; Hugenholtz et al., 2009). Modified suspended sand can be transported as far as 300 m beyond the foredune, with significant amounts of sand, $2-5\ kg/m^2$ in six months, being deposited behind the foredune (Anderson and Walker, 2006). Recent work by Bodenbender et al. (2025) further demonstrates that turbulence can sustain suspended sand transport, with detectable deposition at least 200 m inland. Under strong wind conditions, the suspended flux can be as high as 20% of the saltation/creep flux (Bagnold, 1941), depending on factors such as sediment texture and surface roughness (Nickling and Davidson-Arnott, 1990). Walker (1999) concluded that 15% of the crest transport is deposited on the interdune surface downwind of the dune crest.

High sand fluxes have been observed downwind of foredune notches, reflecting differences in aeolian transport processes between notched and unnotched foredune systems. Riksen et al. (2016) demonstrated higher sediment fluxes downwind of notched foredunes on Ameland (The Netherlands) compared to adjacent unnotched foredunes, although this effect decreased rapidly and became negligible beyond 60 m from the foredune. On the neighbouring island of Terschelling, aeolian sand deposition was found to be restricted to 80 m landward from the vegetated foredune (Riksen et al., 2016). Comparable spatial limits have been reported for unnotched/vegetated foredunes, where aeolian sand deposition is limited to 120–130 m landward of the highwater line (~50–160 m from the foredune crest) (Stuyfzand et al., 2010), and suspended sand cloud reaches ~100 m inland from a vegetated foredune in New Zealand (Petersen et al., 2011).

In contrast, foredune notches generate zones of accelerated wind flow, enhancing sediment transport capacity towards the dune hinterland. Field and modelling studies show that notch geometry and incident wind angle control the wind acceleration and sediment transport rates, promoting sediment transport pathway into the dune hinterland through foredune notches (Nguyen et al., 2021; Nguyen et al., 2022). Consistent with this, studies of blowouts indicate efficient landward sediment transport, with approximately 50% of eroded sediment deposited within 90 m behind blowouts and the remaining 50% transported farther downwind (Baird et al., 2021). Deposition downwind of blowouts decrease exponentially with distance, with detectable aeolian input that extends to at least 200 m inland during strong wind events (Arens et al., 2004; Bodenbender et al., 2025).

To quantify suspended aeolian transport beyond zones of visible geomorphological change, sand traps are proven to be a useful tool, although long-term (multi-annual scale) records are rare. In this study such a multi-annual dataset of sand traps is used. Sand traps already provided insights into how transported sand affects vegetation, soil fauna, and soil composition (Arens et al., 2012; Arens et al., 2013b). At several locations in the Dutch coastal dunes, sand traps have demonstrated that sand can be transported over 300 m in vegetated dunes and over 500-600 m inland from dynamic dunes (Arens et al., 2012; Arens et al., 2013b). The sand particles can be transported in suspended state, possibly due to a speed-up of turbulent wind flow over the topography of a foredune, increasing the sand transport capacity of the wind, a process referred to as 'jettation' (Arens, 1994; Arens et al., 1995; Hesp, 2002; Hesp et al., 2013; Hesp and Smyth, 2016). Using sand trap monitoring over longer time period could prove useful for understanding the impact of remobilizing coastal dune systems on aeolian sand transport.

This study focuses on spatiotemporal suspended aeolian sand transport in relation to the effects of dune remobilization in the Zuid-Kennemerland area. After the construction of a series of notches and reactivated parabolic dunes in the winter of 2012–2013, 15 sand traps were installed to monitor the suspended aeolian sediment flux. These sand traps have been actively monitored over a period spanning ten years.

The aim of this research is three-fold:

1. To study the spatial- and temporal (inter- and intra-annual) variability of the suspended aeolian sand transport, using 15 sand traps at different distances from the foredune, and assess the relation between suspended aeolian transport, meteorological conditions and geomorphological changes,
2. To assess the long-term implications of dune remobilization on spatiotemporal trends in aeolian sediment transport,
3. To understand the importance of suspended sand transport in vegetated dune systems.

2. Research area

The 350 km-long Dutch coastal dune zone can be subdivided into two main districts based on flora types (Van Soest, 1929) and sand composition (Eisma, 1968; Klijn, 1981; Kooijman, 2004) (Fig. 1 A). The Renodunal district, south of the village of Bergen, consists of carbonate-bearing sands supplied by the Rhine and Meuse river system (Eisma, 1968; Schendelaar, 1984). These sands contain both biogenic and detrital carbonate clasts. The Wadden district, north of Bergen, is characterized by carbonate-poor sands, derived from the reworking of sediment deposited by a former Baltic river (Eridanos) system and Saalian glacial deposits of the Pleistocene (Eisma, 1968; Gibbard, 1988). The difference in carbonate content between the two districts is significant: the Renodunal district has 2–10% carbonate, while the Wadden district has a maximum of 2% carbonate (Eisma, 1968; Kooijman, 2004).

The study site is located in the Noordwest Natuurkern, part of the Nationaal Park Zuid-Kennemerland south of the town of IJmuiden, the Netherlands (Fig. 1B). The area belongs to the Renodunal district and

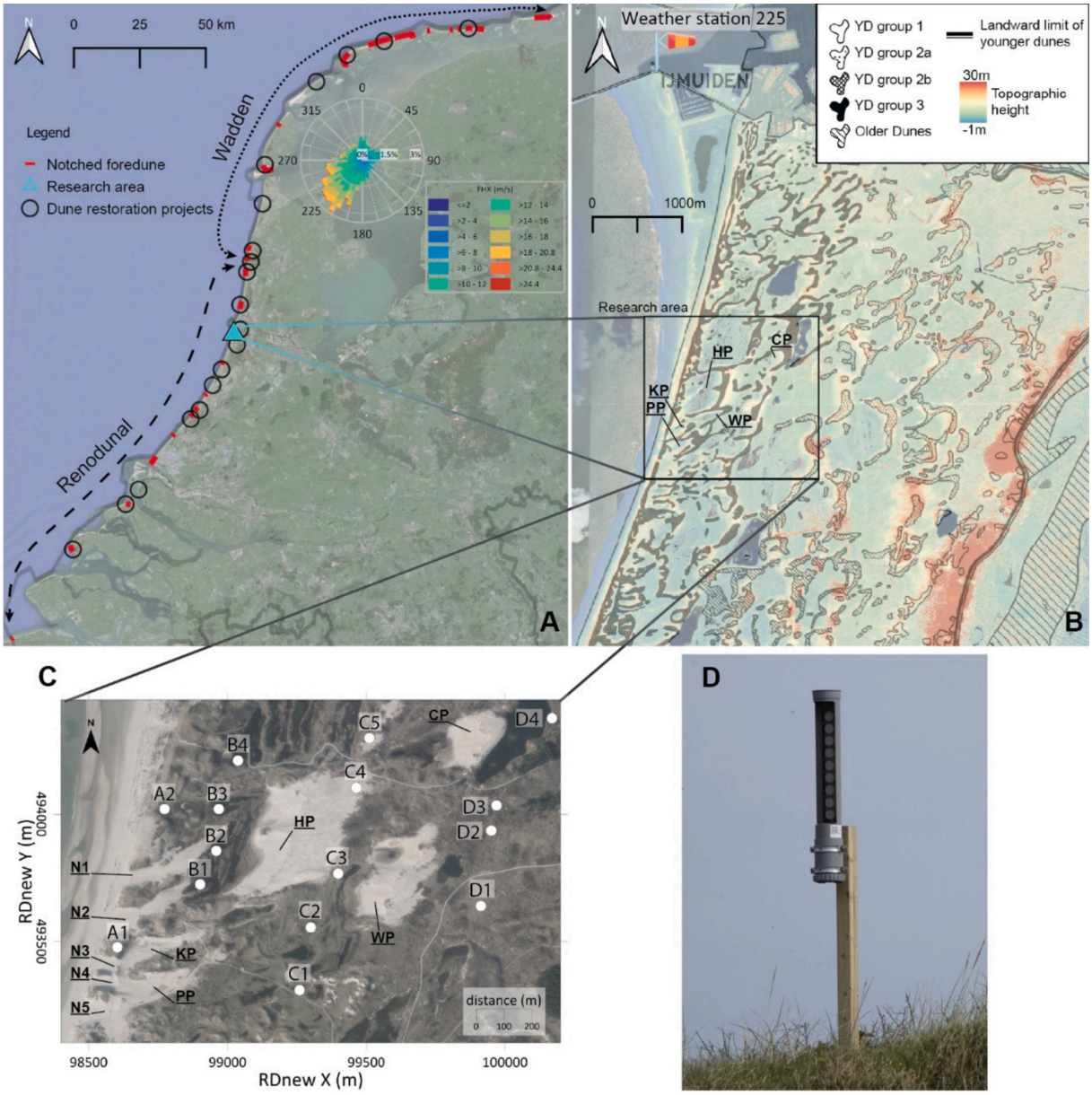


Fig. 1. Overview of the fieldwork area. **A**) map of the Netherlands showing the subdivision of the Dutch coast in the Renodunal and Wadden districts. The red areas indicate notches in foredunes based on publicly available data from 2017 by Rijkswaterstaat. The circles indicate areas where dune restoration projects have been implemented in the Dutch coast, the locations are based on data by Arens (2013a). The blue triangle indicates the research area of this study. The wind rose for the period 2013–2023 is also displayed **B**) zoomed in map of the geomorphology of the research area. The color scale indicates the topographic height, based on data from AHN. The map also shows the different dune deposits found in the research area, modified after Jelgersma et al. (1970). **C**) Satellite image of the research area showing the locations of the sand traps used in this study (A1-D4), indicated by the white dots. Also, the location of the five foredune notches (N1–5) and abbreviations of the reactivated parabolic dunes are depicted in B and C. Abbreviations are PP: Peperedel parabolic dune, KP: Kattendel parabolic dune, HP: Houtglop parabolic dune, WP: Wieringen parabolic dune and CP: Cremermeer parabolic dune. **D**) A sand trap used in this study.

features foredunes, parabolic dunes and deflation plains (now wet dune slacks). The parabolic dunes, known as the Younger Dunes (YD), overlie older beach barrier deposits in the east, called the Older Dunes (OD) (Jelgersma et al., 1970) (Fig. 1B). The sediments in the study area are characterized by carbonate-bearing aeolian sand with a particle size typically ranging from 105 to 210 μm (TNO-GDN, 2025). Based on the morphology of the YD parabolic dunes, a WSW/ENE transport direction can be deduced, compared to the current prevailing wind direction of SW/NE (Jelgersma et al., 1970; Van Straaten, 1961).

In 2011, an EU-funded project (Dutch Dune Revival LIFE: LIFE09 NAT/NL/000418) started in the Noordwest Natuurkern (Ruessink et al., 2018; Kuipers et al., 2016a,b). The project aims to rejuvenate dune habitats and to promote and protect biodiversity. To increase the transport of sand towards the hinterland, five foredune notches were excavated and three large parabolic dunes were reactivated, by removing vegetation, in the winter of 2012–2013 (Fig. 1C). The Houtglop parabolic dune was the largest reactivated dune (Fig. 1C). After the intervention, 15 sand traps were installed in the area (Fig. 1C, 1D). Fig. 2 provides an overview of the study area in 2023.

The foredune notches have been studied in detail over the past decade due to their importance for coastal protection and water safety (Hallin et al., 2019; Kuipers et al., 2016a; Ruessink et al., 2018; Ruessink et al., 2024; Van Kuik et al., 2022; Van Westen et al., 2024). Initial findings by Kuipers et al. (2016a) indicated the project was successful: approximately 45,000 m^3 of sand was deposited behind the foredunes between 2013 and 2015, with 25,000 m^3 originating from erosion of the



Fig. 2. Overview photos of the western part of the study area taken in November 2023. A) overview photo taken in western direction from the southern part of the Houtglop parabolic dune (HP). Notch 1 and 2 (N1 and N2) are indicated together with their depositional lobes by the white dashed line. Sand trap B1 is indicated by the red arrow. B) a photo taken in northeastern direction, towards IJmuiden, from the foredune between notches 2 and 3. The depositional lobes of N1 and N2 are indicated again with the white dashed line. The black line shows the outline of the Houtglop parabolic dune. Behind the Houtglop parabolic dune a part of the Cremermeer parabolic dune (CP) is indicated by the black dashed line. Red arrows indicate sand trap B1 and B2. C) a photo taken from the southern part of the Houtglop parabolic dune towards the southeast. The photo shows the area without notches and RPDs. Here, the grass encroachment is clear, no bare sand bodies are visible. D) a photo of the depositional lobe of notch 5 in the southwestern part of the study area. The photo was taken in northern direction in May 2023. The depositional lobe formed over a cycle path in the dunes, which is not accessible anymore due to the sand.

notches and 20,000 m^3 imported from the beach through the notches. In 2013–2016, multiple sandy depositional lobes formed reaching lengths up to ~150 m (Fig. 2 A, 2B, 2D). The largest RPD (Houtglop parabolic dune) showed an expansion of the deposition zone of approximately 70 m in a NE direction from 2013 to 2016.

Ruessink et al. (2018) concluded that in the first three years following excavation there was an increase in erosion, transport, and deposition of sand. New dune landforms emerged, the area of bare sand

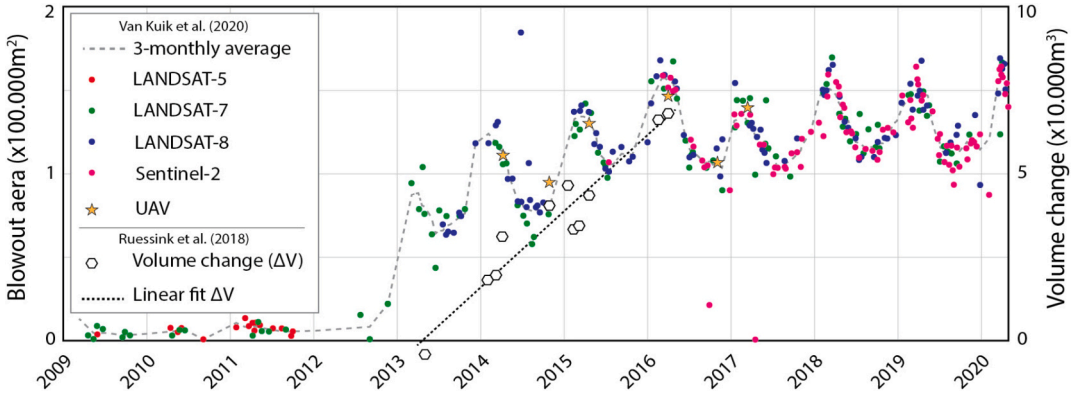


Fig. 3. Data from Ruessink et al. (2018) and Van Kuik et al. (2022) showing the volume change (10,000 mˆ3) of the area behind the notches and the related blowout area (100,000 mˆ2). The volume changes between 2013 and 2016 show a linear increase over time. This increasing trend is also visible in the blowout area between 2013 and 2016 but is followed by a stabilizing trend from 2017 to 2020.

expanded, and there was a positive sand budget landward of the foredune. Most erosion occurred along the sides of the notches, and depositional lobes developed downwind of the notches. While the total sand volume in the study area remained stable post-notch creation, 75% of the sand was deposited landward instead of seaward, indicating the effectiveness in sand transfer to the hinterland. The volume changes of the sandy lobes show a linear increase in the first three years (Fig. 3; Ruessink et al., 2018). The features studied by Ruessink et al. (2018) are mainly attributed to saltation transport of sand, with visible geomorphological changes and bare sand surfaces. A follow-up study using remote sensing data (Van Kuik et al., 2022) showed an overall stabilization in depositional area behind the notches, with seasonal variability between 2013 and 2020 (Fig. 3), also related to saltation transport. The variability is attributed to seasonal cyclicity of vegetation cover and density. A sediment transport model (AeoLiS) applied to the notches shows a similar stabilization of the depositional area over time from 2013 to 2023, with limited negative volume changes at the foredune, and constant erosion of the foredune notches (Van Westen et al., 2024). This model only includes saltation transport as main driver of the dune system.

To monitor suspended aeolian sand transport, which is not measurable using the methods mentioned above, 15 sand traps were placed in the area after the excavation of the notches and RPDs on October 8, 2013 (Kuipers et al., 2016; Fig. 1C and 1D). These sand traps have been emptied over the past decade and their use continues. This rare, multi-annual post-intervention dataset allows suspended aeolian sand transport to be quantified over spatial scales extending beyond zones of visible geomorphological change, and enables assessment of how suspended aeolian transport responds to meteorological conditions and geomorphological changes through time.

3. Materials and methods

3.1. Sand traps and data collection

The sand traps were adapted from Leatherman (1978), and consist of an 80 cm PVC pipe mounted at a middle height of approximately 1.5 m above ground level (Fig. 1D). The centre of their 180° opening is oriented into the dominant southwestern wind direction. At the back of the pipe a 106 μm mesh allows air to flow through while trapping particles. Designed to collect modified saltation- and suspended aeolian sand, the traps are positioned above the saltation zone and placed in vegetated areas where saltation transport is minimal or absent. Their height also reduces the influence of vegetation.

The sand traps were placed in four rows (A, B, C and D) at increasing (perpendicular) distances from the foredune (Fig. 1D). The A1 and A2 sand traps were placed on top of the foredune, with A1 located between two notches and A2 on the unnotched foredune. Sand traps B1–4 are positioned with a perpendicular distance of approximately 300 m from the foredune in a SSW-NNE orientation, parallel to the foredune, with an interval of approximately 200 m between the traps. Traps B1 and B2 are situated downwind of a notch in the foredune, B3 and B4 behind the unnotched foredune.

At a distance of approximately 700 m from the foredune, five C sand traps (C1–5) were placed with a parallel orientation to the foredune. The traps are spaced approximately 300 m apart. Traps C3 and C4 are situated behind the reactivated Houtglop parabolic dune, C1 and C2 behind the notched foredune and C5 behind the unnotched foredune. The most distal sand traps, D1–4 were placed 1200 m in the hinterland, irregularly spaced with distances of 100 to 300 m apart. Trap D1, D2 and D4 are positioned behind the Wieringen and Cremermeer RPD's created in the hinterland, D3 is positioned between the parabolic dunes. Between the Cremermeer RPD and sand trap D4 a perennial lake is present.

Sand traps were emptied over a period spanning from October 2013 to December 2023. Samples were collected in plastic sample bags placed at the bottom of the sand traps. A weight was added to each sample bag to prevent it from turning inside out and spilling the sample due to eventual turbulent wind forces. The A-, C- and D-traps were emptied very regularly without many large data gaps related to malfunctions or logistical problems. In contrast, the B-traps were sampled less regularly due to extensive periods with high water tables in the dune slack where the traps are situated. The longest period a trap collected sand due to inaccessibility spans almost two years (93 weeks). This sample was nonetheless included in the cumulative sediment calculations over the ten-year period. Some intervals lack data due to technical issues with the trap itself. Trap B3, for example, was not operational for 27 weeks in 2020 because the trap was damaged by the free roaming Highland cattle. These intervals are also depicted in the results section of the sand trap data.

After sample collection, the samples were dried on a hotplate before weighing. Occasional remains of vegetation were included in this procedure. Sample weight data is plotted as raw weight (grams) and cumulative weight (grams). The percentual sample weight collected per sampling period ((sample weight/total weight)*100%) referred as sediment contribution, was calculated for each period. The average grams per day per period (sample weight/days within period) referred to as suspended load was calculated as cumulative percentages to better compare different sand traps and sampling periods. Spatial distribution of cumulative yearly weights (gram) was visualized using Surfer by Golden Software, with kriging interpolation used to interpolate between the sand traps. The kriging interpolation was performed in a direction of 45 degrees and tolerance of 45 degrees to account for general wind direction. No data was assigned outside of the convex hull.

3.2. Meteorological data

The dataset provided by Ruessink et al. (2024), containing ten-minute resolution wind speed and direction data from the KNMI (Royal Netherlands Meteorological Institute) weather station 225, was used. This weather station is situated four kilometres north of the study area on a breakwater near the city of IJmuiden (Fig. 1B). The data was obtained using an anemometer and windvane.

From this dataset the daily maximum hourly average wind speed (FHX, in m/s), together with the weighted vector average wind direction (DDVEC in degrees) was calculated for the interval 8 − 10-2013/05 − 12-2023. The KNMI classifies average hourly wind speeds (FHX) between 20.8 and 24.4 m/s as ‘storm’, and hourly wind speeds exceeding 24.4 m/s as ‘severe storm’.

Due to malfunctions of the equipment of different timespans (10 min to 3 days) a total of 14 days do not have FHX values and a total of 130 days do not have the vector average wind direction values. These values are replaced with rectified daily values of weather station 225 provided by the KNMI that contain validated information for these days, thus completing the dataset.

Wind data and sand trap data over the ten year interval are compared to deduce temporal trends in suspended sediment transport in relation to meteorological conditions.

Additionally, drift potential (DP) was calculated following the Fryberger framework (Fryberger, 1979; Pearce and Walker, 2005) using unclassified, the 10-min wind data measurements. For each timestep, winds with velocity V (m/s) exceeding a threshold velocity V_t (m/s) were weighed according to $Q \propto V^2(V - V_t)$, to estimate a relative sediment transport potential (drift potential) (Q), while sub-threshold winds contribute zero. Drift potential was aggregated into 22.5 degrees wind-directional sectors, while resultant drift potential (RDP) and resultant drift direction (RDD) were obtained from vector summation into the transport direction. The robustness of transport orientation and directionality were tested using varying threshold velocities (6 m/s, 7 m/s, 20.8 m/s). Threshold velocities of 6 m/s and 7 m/s were selected to represent commonly applied lower bounds for aeolian transport, capturing moderate transport conditions, while the 20.8 m/s threshold

isolates storm-dominated transport. Using a high-frequency long-term unclassified wind dataset results in higher PD values compared to values reported in classical Fryberger studies. DP is therefore treated as a relative, internally consistent measure, rather than a comparable index. Interpretation focuses on RDP/DP as an indicator of directional variability and RDD as the dominant transport orientation.

3.3. Satellite imagery and digital elevation models

Desaturated (grayscale) infrared satellite images from the Netherlands Space Office (NSO) were used to create yearly timelines of bare sand area for comparing sand trap data with the morphological evolution (migration of bare sand bodies) in the study area. This method is based on work by Arens and Van Dijk (2025). The specific satellite and image resolution is shown in Table 1. The images were processed and correlated with yearly cumulative suspended load data using Surfer by Golden Software. In order to correlate the morphological changes to spatial yearly flux trends, the satellite images of each specific year are overlain by the yearly cumulative weight kriging maps of the sand trap data.

In order to better understand the dynamics, digital elevation models are used to map erosional- and depositional patterns. Digital elevation models (DEM), publicly available data from the Current Dutch Elevation (Actueel Hoogtebestand Nederland/AHN) dataset were used, AHN3 (January 2014), AHN4 (April 2020) and AHN5 (December 2022–January 2023). The grid cells have a size of 0.5 × 0.5 m, with a maximum standard height error for AHN 3 and 4 of 5 cm and for AHN5 3 cm. The method used in this study is also inspired by Arens and Van Dijk (2025). The elevation models were subtracted using Surfer by Golden Software to create elevation change maps, showing erosion and deposition for the periods 2014–2020 (AHN4–3) and 2020–2023 (AHN5–4) in meters. The volume calculations were generated for each grid cells (0.5 m × 0.5 m) within a polygon. If the surface was tilted at the top or bottom of a grid cell, the volume of the prism at the top or bottom was approximated for the grid cell column. Volume changes were calculated for the five notches (combined) and the three separate RPD's in the hinterland in m^3/year. The elevation change maps and volume calculations were used to correlate the spatiotemporal suspended sand transport to geomorphological changes (erosional- and depositional patterns).

4. Results

4.1. Geomorphological evolution of notches and RPD's (2013−2023)

4.1.1. Aerial expansion of depositional lobes

Satellite imagery was used to trace bare sand bodies annually, resulting in yearly timelines showing expansion (Fig. 4). The timelines show differences in bare sand area expansion between the different notches and RPD's. The northernmost foredune notch (N1) shows rapid downwind expansion between 2013 and 2017, followed by a decrease in expansion up to 2023. In 2017, the depositional lobe reached a waterbody, limiting further visual tracking. Similar to N1, N2 shows a rapid expansion from 2013 to 2017. The depositional lobe entered the waterbody in 2020. The area expansion of N2 is approximately half that of N1. Both depositional lobes can also be seen in Fig. 2 A and 2B.

In the south, N3, N4 and N5 show complex patterns. Within the first three years, the area expands and connects with either the Kattendel parabolic dune or the Peperedel parabolic dune. After this connection, the expansion is limited, also for the Kattendel and Peperedel parabolic dunes. For N5, the area does expand after 2017, but the expansion is oriented towards the southeast, and stagnates after 2021. This southeast expanding depositional lobe blocks a cycle path (Fig. 2D).

The Houtglop parabolic dune shows a constant yearly downwind expansion up to 2019. After 2019 the northern part of the Houtglop parabolic dune expands faster compared to the southern part. From 2021 onwards sand trap C4 is located in the bare sand area.

The Wieringen parabolic dune shows four distinct depositional lobes. The two northern lobes expand up to 2021. Afterwards no changes are observed. The two southern lobes are still active in 2023. During the first two years these sandy lobes expanded, followed by a decrease in expansion until 2021. In 2022 expansion increased, especially in the upper lobe.

The Cremermeer parabolic dune is situated on the bank of the perennial Cremermeer lake, making it difficult to observe an eastward expansion, since most of the sand deposits into the lake. The bare sand area mainly expanded between 2013 and 2016. Afterwards, expansion seemed to decrease, but continued towards the east up to 2023.

The yearly timelines show changes in dynamics in the area, N1 and N2 show expansion of the bare sand area between 2013 and 2023, while N3–5 show stagnation of areal expansion. The Houtglop parabolic dune shows continuous expansion while the other two parabolic dunes show variations throughout the study period.

4.1.2. Volumetric calculations

The elevation (geomorphological) changes between 2014 and 2020 and 2020–2023 are depicted in the DEM maps in Fig. 5, together with the polygons used for volumetric calculations and their values. These values are also shown in Table 2. Blue areas indicate erosion and red areas indicate deposition. At the notches, the walls are eroding, increasing the width of the notch. The maximum erosion rates surpass three meters in the period 2014–2020 (>0.5 m/year). Sand is deposited directly behind the landward opening, surpassing positive elevation changes of three meters (>0.5 m/year). Similar to the notches, elevation changes of 3 m occur at the RPD's, where erosion affects the upwind faces of the RPD. Deposition is concentrated downwind, forming depositional lobes adjacent to the erosional areas.

During the period 2020–2023, erosion shifted from being localized in the notches and RPD's, including erosion of notch floors and walls, towards erosion of the depositional lobes and downwind progradation of the depositional area, forming active parabolic dune features. This shift is especially evident behind the Houtglop parabolic dune. Compared to the 2014–2020 period, erosion of notch walls was reduced. However, maximum local erosional- and depositional rates within the notches and RPD's (>0.5 m/year) showed no systematic change between the two periods, indicating sediment reworking was maintained, despite spatial redistribution of erosional and depositional zones.

Volumetric calculations also reveal a shift in sand budget dynamics between the two periods. From 2014 to 2020 the positive mass balance (+12,216 m^3/year; Table 2) in the polygon surrounding the notches indicates an import of sand from the beach. All RPD's, however, show a negative mass balance. This negative mass balance indicates that a fraction of the eroded sand is not retained within the depositional lobe or polygonal area, but is transported farther downwind. In the period 2020–2023 the mass balance of the notches still shows an import of sand into the hinterland with comparable volumes. Less erosion occurs on the notch walls, resulting in a higher positive mass balance (+14,975 m^3/

Table 1
List of NSO satellite imagery used in this study with the corresponding date, satellite name and resolution.

Date	Satellite	Resolution
10/10/2014	Spot 6_7	1.5 m
27/10/2015	Spot 6_7	1.5 m
16/10/2016	Spot 6_7	1.5 m
16/10/2017	TripleSat	0.8 m
27/09/2018	TripleSat	0.8 m
03/09/2019	SuperView-1	0.5 m
09/11/2020	SuperView-1	0.5 m
04/11/2021	SuperView-1	0.5 m
22/09/2022	SuperView-1	0.5 m
28/11/2023	Pleiades-NEO	0.3 m

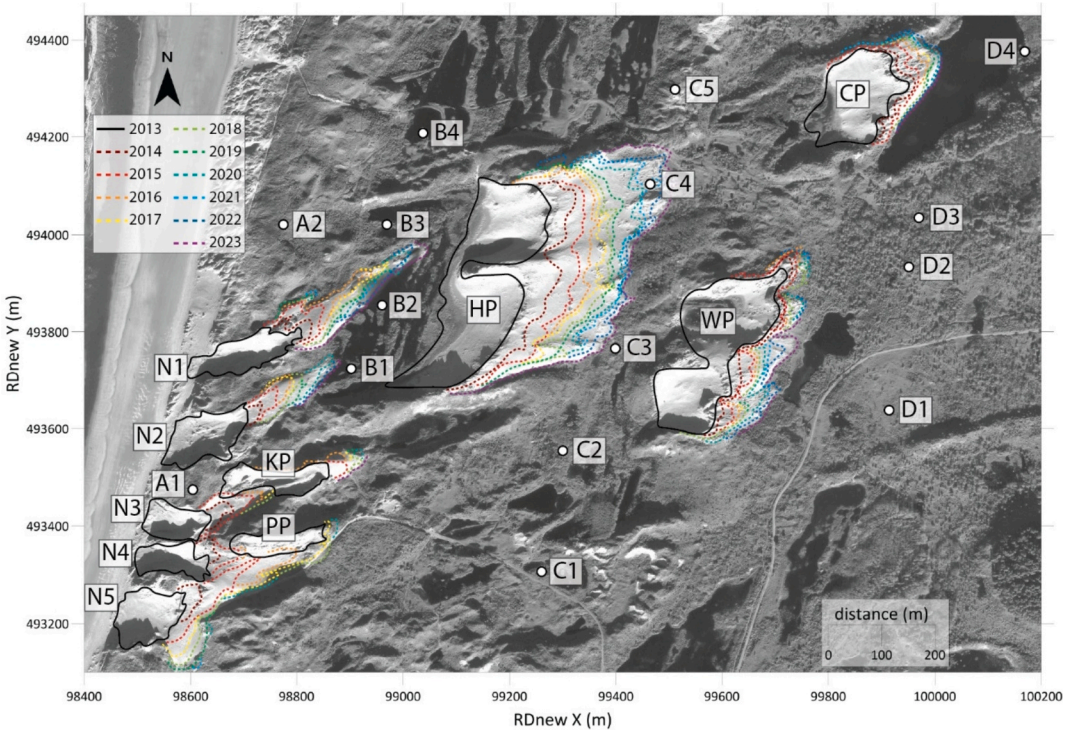


Fig. 4. Satellite imagery of the research area where the depositional sand lobes behind the notches and RPDs have been traced each year. On the map the original shape of the excavation in 2013 is indicated in black. The location and name of the sand traps (A1-D4) are also shown. The notches are indicated by N1-N5, the Houtglop parabolic by HP, Wieringen parabolic dune (WP) and the Cremermeer parabolic dune (CP).

year). In contrast to the previous period, the Houtglop and Wieringen parabolic dunes also show a positive mass balance (+1314 and + 360 m^3/year respectively), suggesting import of sand. The Cremermeer parabolic dune still shows a negative mass balance (−441 m^3/year), albeit more than halved.

The decrease in expansion of bare sand areas behind the notches does not imply that there is a decrease in sand transport. To the contrary, the dunes remain dynamic throughout the full study period 2013–2023. The biggest change in the study area is shown at the reactivated parabolic dunes, here a change occurred from a negative mass balance in 2014–2020 to a less negative (Cremermeer RPD) or positive (Houtglop- and Wieringen RPD) mass balance in the period 2020–2023.

4.2. Suspended sand and meteorological data 2013–2023

4.2.1. Sample weights and cumulative weights

Suspended aeolian sand transport occurs throughout the study area, with measurable sediment capture in all sand traps. Although cumulative suspended sand loads generally decrease downwind, reflecting distance from the sediment source and reduction of landform size and wind driven transport capacity, episodic wind events transport suspended sand across the dune system. Fig. 6 presents biweekly and cumulative suspended sand capture recorded for all 15 sand traps from October 2013 to December 2023. Traps located on the foredune generally record the high cumulative loads of several kilograms, while more distal traps show lower overall accumulation of hundreds of grams. However, several traps do not fit within this distance-based gradient. Particularly the traps downwind of notches and RPD's (e.g. B1, C4 and D4) captured high cumulative loads, despite their distance from the foredune. Table 3 summarizes cumulative weight, average biweekly weight, peak sample weight, the sample collection date and the period in weeks over which the peak weight was captured.

The sample weight data shows episodic peak transport, resulting in steps in the cumulative curve. A storm triplet in February 2022 resulted in the most prominent transport event, with peak weights recorded in nearly all sand traps (Fig. 6). Based on the cumulative curves, differences in temporal trends are observed between traps with similar distances to the foredune. The sediment data were compared to the meteorological wind data from weather station 225, to explain the different peaks.

4.2.2. Meteorological data

Meteorological data from weather station 225 support the aforementioned dominant wind (and resulting sediment transport) direction in the study area, with an average vector wind direction of 235.3 (SW) degrees in the period of October 2013–2023 with FHX (daily maximum hourly average wind speed) values ranging from 3.1 m/s to 30.1 m/s and an overall average wind speed of 10.4 m/s. In total, 35 storms (FHX >20.8 m/s) were recorded at weather station 225 (Table 4). The storm duration ranges between one to twelve hours. Wind direction during storms ranged between SSE and NW, allowing suspended sediment to be collected through the SW oriented opening of the sand traps.

The 35 storms occurred mostly during the autumn and winter seasons (Table 4). A total of seven severe storm events (FHX, >24.4 m/s) occurred in this period in the study area (Table 5). To investigate the relation between storminess and aeolian suspended sediment transport, the sediment contribution and percentual suspended load data is plotted with the meteorological data.

The Fryberger drift potential analysis indicates a consistently NEE-directed (~59°) resultant drift direction (RDD) and predominantly unimodal wind regimes, with RDP/DP values exceeding 0.66. Results obtained using different threshold velocities are summarized in Table 6 and Fig. 7. Increasing the threshold velocity results in only minor changes in RDD (<1°), while RDP/DP values increase from 0.66 to 0.86. These results indicate a stable transport orientation and a highly directional wind regime, with transport increasingly dominated by rare storm events at the 20.8 m/s threshold value. Notably, six sand traps (A2, B3, B4, C1, C2 and D4) are not located downwind of an active erosional surface in the RDD, indicating that suspended sand capture cannot be attributed solely to lee-side trapping behind eroding faces of notches and

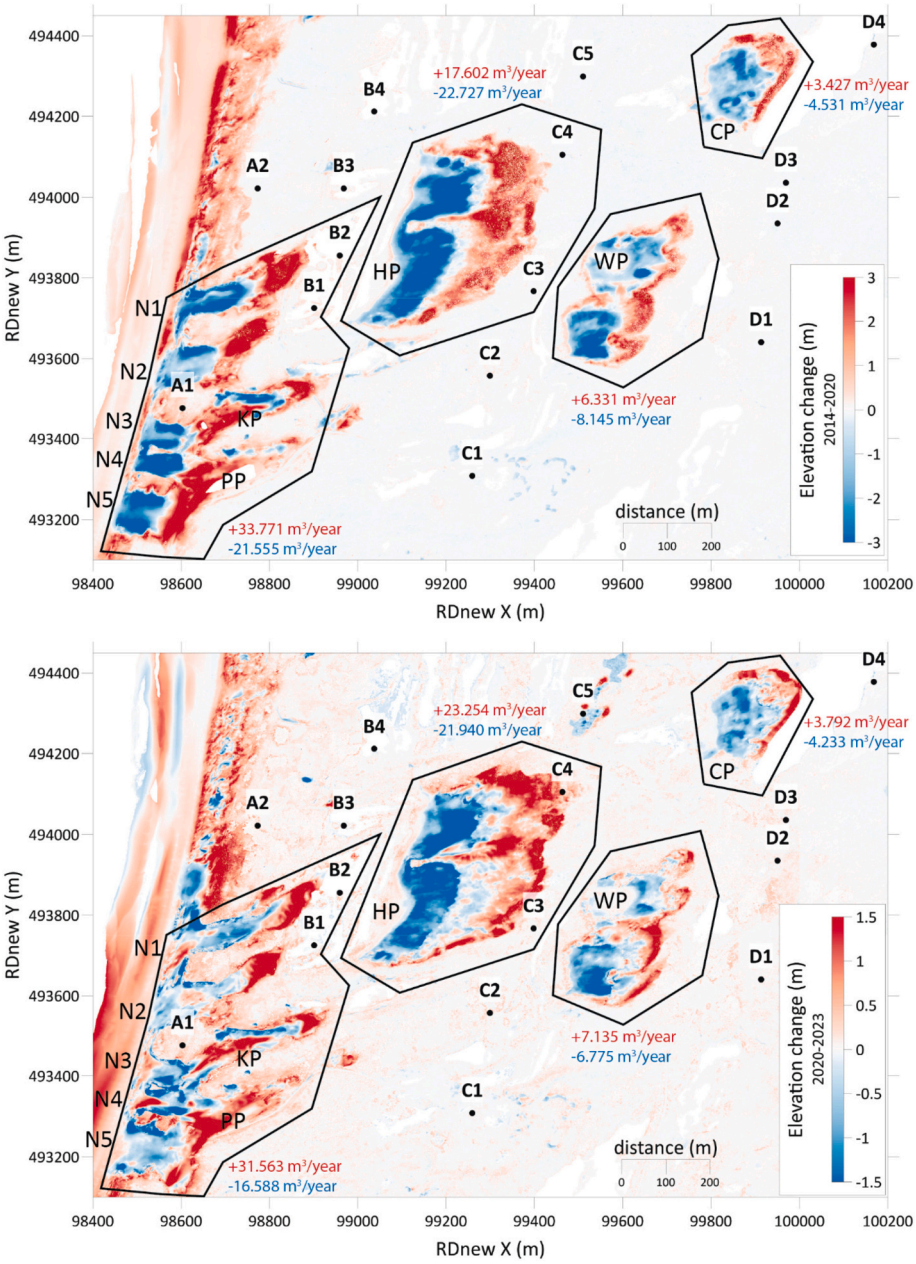


Fig. 5. Two maps of the research area showing positive (red) and negative (blue) surface level changes based on DEM map calculations in meters. The polygons show areas for which volumetric changes were calculated in mˆ3/year. The top map shows the difference between AHN4-AHN3 between 2014 and 2020. In the bottom map the height and volume difference of the period 2020–2023 (AHN5-AHN4) are shown. The notches are indicated by N1-N5, the Houtglop parabolic by HP, Wieringen parabolic dune (WP) and the Cremermeer parabolic dune (CP).

RPD's.

4.2.3. Sediment contribution data

Over the ten-year monitoring period, suspended aeolian sand transport was strongly dominated by a limited number of storms. Of the 35 storm events identified, including seven severe storms, these relatively short-lived events account for a large proportion of the total suspended sediment transported across the dune system. The sediment contribution of the sand traps during the severe storm events is shown in Table 7. These percentual values are used to compare the sample weight data from the different sand traps in relation to the storm events. The total sediment contribution during all 35 storm events in the area is also shown in Table 7.

The suspended sediment contribution of individual severe storms are highly variable. Some of these storms show a pronounced increase in suspended load (e.g. storm Eunice), while others only had a minor impact (e.g. 20/11/2015 storm). The spatial contribution of each sand traps is also variable, with relative higher contributions generally observed at the foredune and in the most distal sand trap locations.

The sediment contribution related to the seven severe storms ranges from 17% for trap B3 to 67.8% for trap C3. In seven events in a period spanning over ten years, none of which lasts more than twelve hours, an average of at least 39.7% of the total cumulative weight per sand trap was collected, keeping in mind some sand traps were not operational during storms. The total storm sediment contribution per trap ranged from 31.4% to 88.6% of the total weight.

Table 2
Volumetric changes based on the DEM maps and polygon boundaries. Notches consistently show a positive mass balance, while RPDs transition from a negative to a positive mass balance.

Period 2014–2020	Deposition (m^3/year)	Erosion (m^3/year)	Mass balance (m^3/year)
Notches	33,771	21,555	12,216
Houtglop	17,602	22,727	-5125
Wieringen	6331	8145	-1814
Cremermeer	3427	4531	-1104
Period 2020–2023	Deposition (m^3/year)	Erosion (m^3/year)	Mass balance (m^3/year)
Notches	31,563	16,588	14,975
Houtglop	23,254	21,940	1314
Wieringen	7135	6775	360
Cremermeer	3792	4233	−441

4.2.4. *Suspended load data*

We explored the relationship between sedimentation, wind speed and wind direction (Fig. 8). Storm events are depicted by blue triangles, the individual severe storm events are depicted by the red vertical arrows. The wind direction is shown as daily vector values. The recorded storms, in general, coincide with the steps in the suspended load curve of the period in which the storm occurred. As shown in the previous section, these periods are responsible for up to 89% of the total captured weight in some sand traps. Periods without storms are characterized by flat areas in the suspended load curve.

Although both wind speed and wind direction were highly variable throughout the studied time period, no trend (as indicated by the linear fit of the FHX curve in Fig. 8) is visible, meaning that the overall windiness did not change over time. The wind direction also showed no systematic change over time. During the winter seasons the wind speed increased and mainly shows wind directions between 180 and 360 degrees (S—N). However, looking at the cumulative suspended load curves (Fig. 8), some trends can be discerned in the data. Some sand traps show a decrease in suspended load over time, flattening the curve, such as A1 and B1. Other traps show a stable cumulative increase over time, A2, C1 and D1 for example. An increasing trend over time is also visible, mainly in sand traps C3–5.

4.3. *Spatial suspended sediment transport patterns 2013–2023*

In order to visualize the spatiotemporal suspended sediment transport patterns, the cumulative yearly sample weight data is plotted as

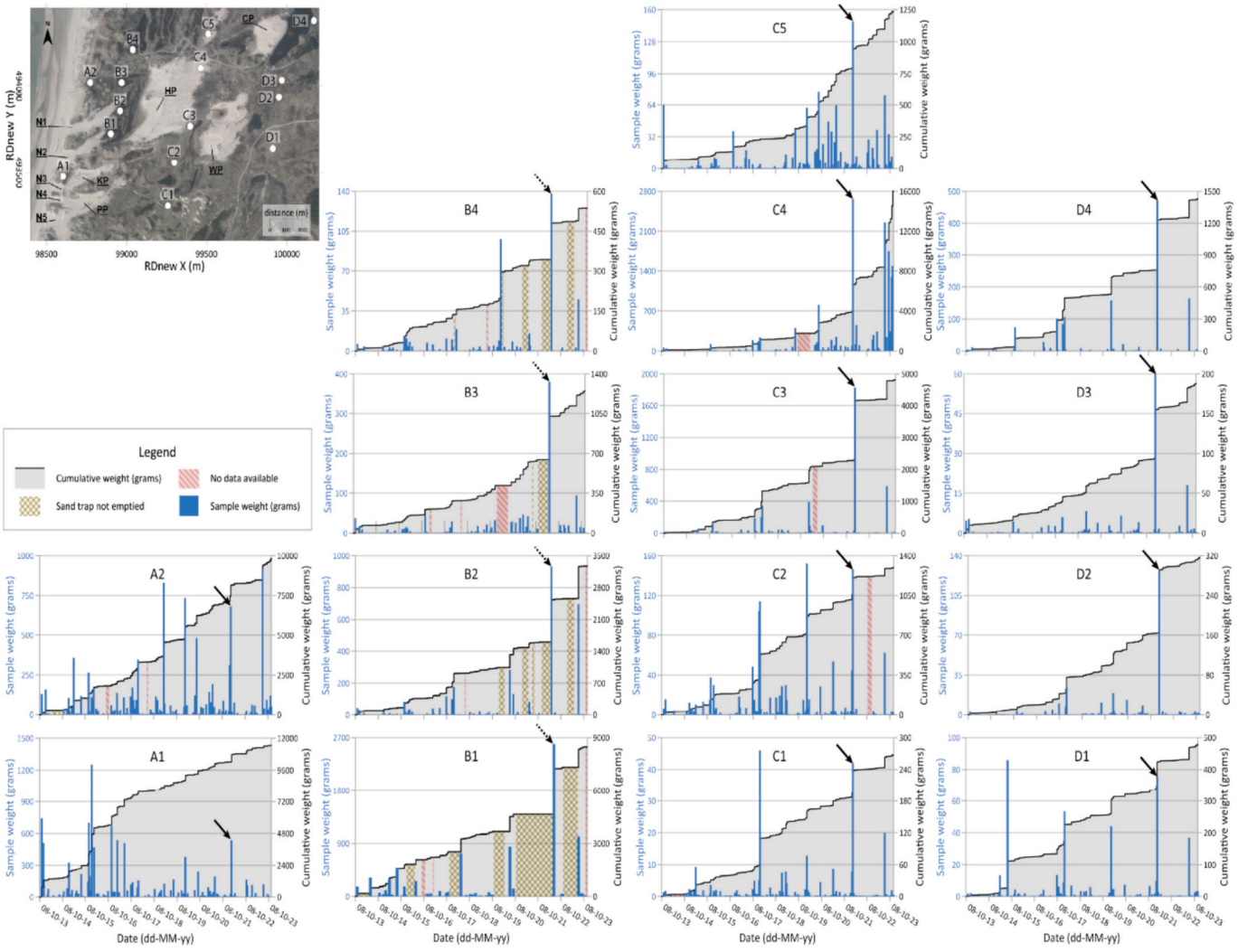


Fig. 6. Sample weight and cumulative weight (grams) of each sand trap plotted against time. Red sections in the cumulative flux indicate periods where sand traps were not operational. Yellow sections highlight periods of extended sediment capture. The map shows the locations of the sand traps in the study area. The black arrows indicate a high transport event present in all sand traps, the dashed arrows indicate the same event in combination with a period of extended sediment capture. Note that both left and right Y-axes vary.

Table 3
Summary of the sand trap data over the period 2013–2023.

Sand trap	Cumulative weight (g)	Average biweekly weight (g)	Maximum captured weight (g)	Max. sample collected (date)	Span max. Period (weeks)
A1	11,457	43.2	1254	19-01–2016	2
A2	9820	37.1	916	19-07-2023	2
B1	8478	32.0	**2594**	**22-06-2022**	**93**
B2	3271	12.3	**932**	**11-05-2022**	**24**
B3	1249	4.7	**380**	**11-05-2022**	**28**
B4	537	2.0	**138**	**11-05-2022**	**24**
C1	268	1.0	46	30-01–2018	2
C2	1296	4.9	152	18-02-2020	2
C3	4814	18.2	1828	22-02-2022	2
C4	16,020	60.5	2665	23-02-2022	2
C5	1235	4.7	148	23-02-2022	2
D1	478	1.8	86	04-08-2015	2
D2	316	1.2	126	22-02-2022	2
D3	188	0.7	60	23-02-2022	2
D4	1430	5.4	473	23-02-2022	2

contour maps overlaying the corresponding satellite image of each year (Fig. 9). The color scale range changes for each contour plot because of the increasing timespan shown in the data. Spatial transport patterns remained relatively stable with high sample weights recorded at the notched foredune (A1), and relatively lower weights at sand trap A2. The B-traps showed a similar pattern where traps B1 and B2 show higher values compared to the northern traps B3 and B4. Over time, starting in 2016, an increase in yearly weight is visible at sand traps C3 and C4, eventually surpassing the amount in the foredune in 2023. Trap C5 also shows this increase in sand capture over time, while traps C1 and C2 remain stable with low sample weights. The D-traps all have low values, comparable with B3–4 and C1.

Initially, suspended transport decreased with distance from the foredune. From 2016 onward, a more complex pattern emerged, with increasing transport behind RPD's. Here, a decrease in transport was observed from the A- to B-traps, followed by an increase from the B- to C-traps and finally another decrease in transport from the C- to D-traps. There are some traps that do not follow this general pattern. Sand traps

Table 5
Severe storm events registered at IJmuiden (station 225, KNMI) in the period 2013–2023. DDVEC is the vector average daily wind direction. FHVEC is the vector related average daily wind speed. FHX is the highest hourly average wind speed. FHN is the lowest hourly average wind speed. FXX is the highest wind gust measured.

Date	DDVEC	FHVEC	FHX	FHN	FXX	Name
28/10/2013	224.3	16.5	**27.8**	11.3	38	–
25/07/2015	292.3	10.1	**24.9**	3.2	34	–
20/11/2016	196.4	9.9	**26.5**	4.0	37	–
18/01/2018	258.7	10.8	**27.8**	3.2	37	–
09/02/2020	204.7	18.6	**24.4**	9.4	33	Ciara
18/02/2022	228.7	15.5	**26.7**	5.3	36	Eunice
05/07/2023	247.8	11.8	**30.1**	5.1	41	Poly

Table 6
Fryberger drift potential (DP), resultant drift potential (RDP), resultant drift direction (RDD) and RDP/DP ratio calculated for three threshold wind velocities. Lower thresholds represent moderate transport conditions, whereas the 20.8 m/s threshold isolates storm-driven transport.

Threshold wind velocity (m/s)	DP (vector units)	RDP (vector units)	RDD (°)	RDP/DP
6 m/s	1.96×10^8	1.29×10^8	**58.73°**	**0.66**
7 m/s	1.64×10^8	1.12×10^8	**58.50°**	**0.68**
20.8 m/s	1.02×10^6	8.77×10^5	**59.4°**	**0.86**

B3 and B4 showed a stronger decrease in transport compared to traps B1 and B2. Traps C1 and C2 showed a consistent downwind decrease in transport from the foredune, unlike traps C3–5 that showed an increase in transport. Sand trap D1 also showed a different trend compared to the other D-traps, here a (minor) increase is observed.

The suspended aeolian transport trends described in the previous paragraph, traps B3, B4, C1, C2 and D1 having the lowest sediment input compared to the other traps with similar distances towards the foredune, shows the suspended sand transport in the Kennemerduinen area is variable over space and time.

5. Discussion and conclusion

The amounts of sand that were blown into the dune area surpassed all expectations. The sand traps collected 57,777 g in ten years and have been emptied 222 times, resulting in a detailed long term monitoring of a remobilized dune system. Based on combined geomorphological-, meteorological and sand trap data, clear spatial and temporal differences in suspended aeolian sand transport are identified across the dune system.

The geomorphological data show expansion of the bare sand area behind the notches up to 2017, afterwards expansion is limited. The reactivated parabolic dunes remain active throughout the study period showing a continuous growth in deflation plain upwind and depositional area downwind. The digital elevation models show that the mass

Table 4
Chronological overview of recorded storms and storm duration. Each date corresponds with a separate storm event. The bold dates are a single storm spanning two days.

Storm date	Storm duration (hours)	Storm date	Storm duration (hours)	Storm date	Storm duration (hours)	Storm date	Storm duration (hours)
27-10-2013	1	**17-11–2015**	**5**	10-08-2019	4	20-02-2022	3
28-10-2013	7	07-01–2016	1	09-02-2020	10	21-02-2022	2
05-12-2013	6	08-02-2016	1	11-02-2020	1	05-07-2023	5
23-12-2013	1	28-03-2016	2	**25-08-2020**	**12**	19-09-2023	1
24-12-2013	9	20-11–2016	4	27-12-2020	5	02-11–2023	2
09-02-2014	2	23-02-2017	3	11-03-2021	2		
15-02-2014	1	06-06-2017	3	21-05-2021	2		
12-12-2014	4	13-09-2017	8	31-01–2022	4		
31-03-2015	2	03-01–2018	5	16-02-2022	1		
25-07-2015	3	18-01–2018	5	**18-02-2022**	**12**		

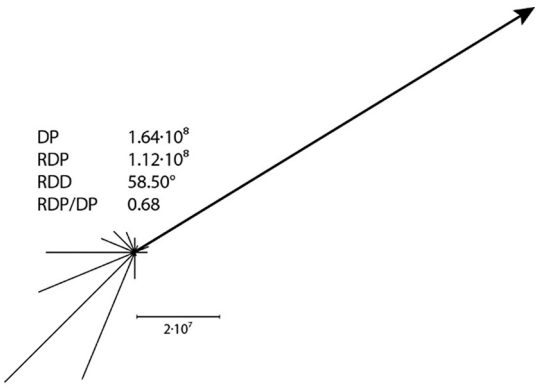


Fig. 7. Resultant drift potential (RDP) vector (arrow) derived from the Fryberger drift potential analysis using a threshold wind velocity of 7 m/s. Drift potential (DP) values are aggregated into 22.5° wind-direction sectors (lines) and vectorsummed to obtain the resultant drift direction (RDD = 58.5°) and RDP magnitude. Associated DP, RDP and RDP/DP values are shown for reference. Scale bar indicates DP and RDP magnitude.

balance at the notches between 2014 and 2020 and 2020–2023 remain relatively stable, while a change occurs from a negative mass balance into a slightly positive mass balance at the reactivated parabolic dunes.

The meteorological data show that storms are the major source, up to 89%, for suspended aeolian sand transport in the study area. Suspended aeolian sand was detected at distances of at least 1200 m inland (sand trap D1), indicating that episodic storm-driven suspension can transport sand beyond zones of visible geomorphological change. The sediment contribution during 35 storms ranges from 31.4% up to 88.6% of the total weight collected over a decade. The suspended load data reveal distinct temporal changes, with linear, decreasing and increasing cumulative loads observed in different morphological parts of the dune system. These trends are not related to long-term changes in windiness or wind direction, but instead reflect differences in geomorphological evolution such as notch widening and the migration of depositional lobes. The observed spatial differences in suspended sand transport reflect the evolving geomorphology of the reactivated dune system. The implications of geomorphological changes, meteorological conditions on changes in spatial suspended sand transport will be discussed in the next section.

5.1. Morphodynamic response to dune remobilization

5.1.1. Geomorphology

5.1.1.1. Notches. The geomorphology exhibits continuous activity and change throughout the observation period (Fig. 5 and 10). Between 2014 and 2020, patterns of erosion and deposition at the notches closely resemble those reported by Ruessink et al. (2018). Erosion predominantly occurs along the notch walls, while deposition is concentrated immediately behind the notches in the hinterland, with depositional rates averaging approximately 0.5 m/year.

Volumetric calculations of the notches in this study (average ~ 32,500 m^3/year deposition and ~ 19,000 m^3/year erosion) are comparable to those reported by Ruessink et al. (2018) (~29,000 m^3/year deposition and ~ 13,000 m^3/year erosion) and Arens and Van Dijk (2025) (average ~ 35,600 m^3/year deposition and 21,100 m^3/year erosion). Differences between these studies are expected, as volumetric results are sensitive to polygon definition and methodological choices. For example, Ruessink et al. (2018) excluded the Kattendel- and Peperedel parabolic dunes, whereas this study includes both parabolic dunes and the notches within a single polygon.

Temporal differences between the studies also play a role. Ruessink et al. (2018) analyzed three years 2013–2016, which partially overlaps with this study's 2014–2020 period with a different elevation dataset. During the following period (2020−2023), the depositional zones behind notches 1 and 2 show signs of erosion. Deposition becomes more localized, migrating downwind towards sand traps B1 and B2. In contrast, notches 3–5 exhibit minimal changes relative to the earlier period. Erosion of notch walls has decreased over time, which Van Kuik et al. (2022) suggested contributes to the reduced lateral expansion of depositional lobes. Despite reduced erosion, deposition rates remain stable (33.771–31.563 m^3/year), indicating continued sand transport to the hinterland. The apparent reduced expansion of the lobes might be related to the infill of the Kattendel and Peperedel parabolic dunes by lobes 3–5 and the infill of the wet dune slack by lobes 1 and 2.

5.1.1.2. Reactivated parabolic dunes. The geomorphology of reactivated parabolic dunes within the study area have been monitored by Arens and Van Dijk (2025). Based on annual growth lines (Fig. 4), depositional areas associated with RPD's expanded consistently from 2014 to 2020, indicating parabolic dune development. The depositional zones have migrated downwind towards sand traps such as C3–5 and D2–4.

Table 7
Percentual sample weight data per trap per severe storm event and the total increase per trap of all storms combined. Missing data is indicated by red dashes. The total sum % and average % values with more than two data gaps is also indicated in red. The maximum values for each trap is displayed in bold. The total sum of the percentual increase during all storms and during the severe storms is shown in the last two rows.

Severe storms (date)	A1	A2	B1	B2	B3	B4	C1	C2	C3	C4	C5	D1	D2	D3	D4
28/10/2013	**6.5**	1.3	2.0	1.3	3.0	1.2	0.5	0.5	0.3	0.4	5.2	0.4	0.9	2.5	0.3
25/07/2015	1.9	1.2	5.8	0.2	0.5	0.2	0.7	1.0	2.0	0.0	0.0	**17.9**	0.1	0.3	0.0
20/11/2016	5.8	0.6	0.6	0.3	3.6	1.4	0.0	0.0	0.0	0.2	3.1	0.0	0.1	0.1	0.0
18/01/2018	1.4	3.5	-	5.4	2.4	-	**17.2**	8.8	7.2	1.5	0.4	11.1	7.6	3.1	7.4
09/02/2020	3.3	7.5	-	-	-	**18.2**	4.8	**11.7**	8.1	0.0	4.9	9.2	6.1	1.5	11.1
18/02/2022	4.7	6.9	-	-	-	-	15.7	11.3	**38.0**	**16.6**	**12.0**	15.6	**39.9**	**31.9**	**33.1**
05/07/2023	1.0	**9.3**	**12.0**	**21.3**	**7.5**	8.4	7.5	4.8	12.2	14.1	6.0	7.7	-	9.6	11.5
Total sum severe storms (%)	24.6	30.3	20.4	28.5	17	29.4	46.4	38.1	67.8	32.8	31.6	61.9	54.7	49	63.4
Total sum all storms (%)	70.7	57.4	31.4	50.2	36.1	47.3	64.7	68.2	85.7	67.1	58.0	77.4	77.8	72.0	88.6

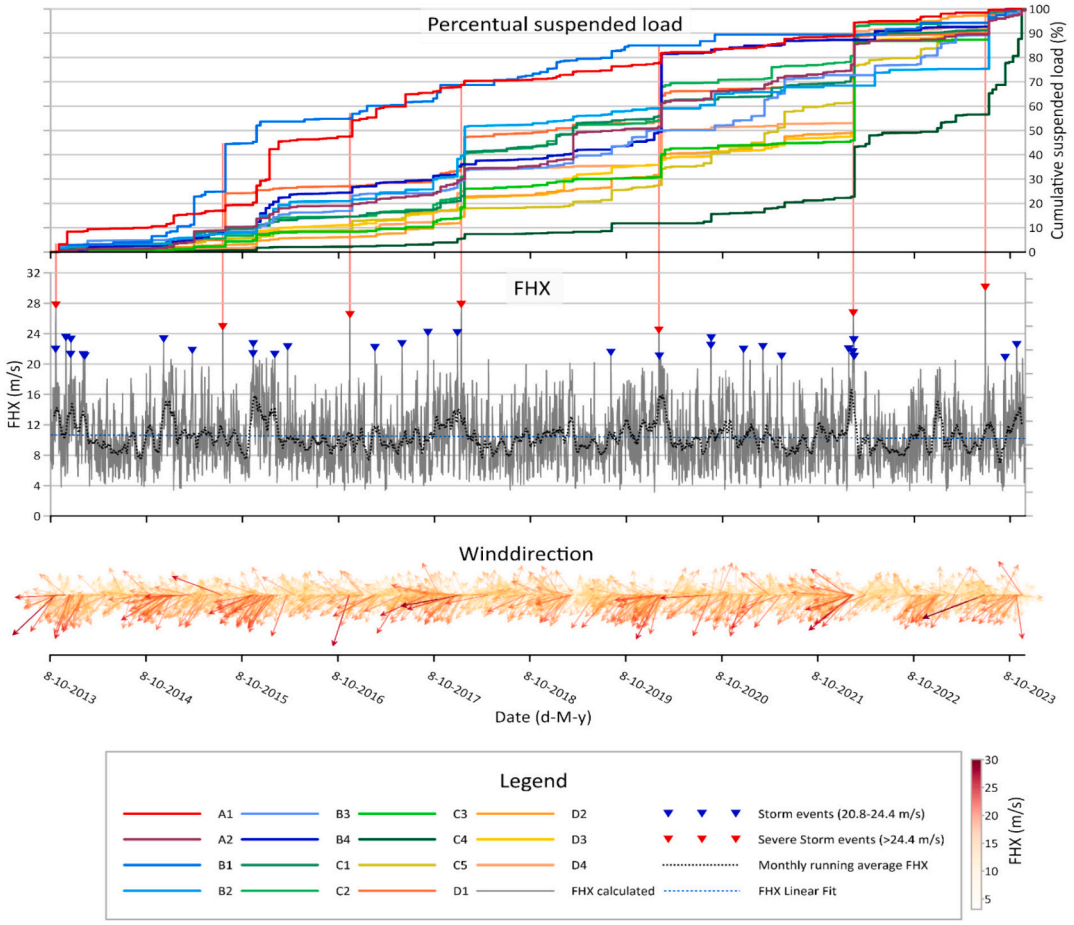


Fig. 8. Cumulative suspended load in percentages per trap and FHX (daily maximum average hourly wind speed) plotted against time. 35 storm events are indicated by the blue triangles. Of these storm events seven are severe storms that are highlighted by the arrows. Together with the storms, the monthly running average is indicated by the black dotted line and the linear trend fit of the FHX data is indicated by the blue dashed line. The wind direction is plotted as vectors with the origin on a baseline corresponding to the specific date. The length and color indicate the wind speed (FHX).

This process of parabolic dune development behind blowouts was also observed by (Hugenholtz and Wolfe, 2006).

Volumetric data shows a transition in RPD behavior, from net erosion (2014–2020) to net deposition (2020–2023). Baird et al. (2021) found that blowouts typically have a negative mass balance, with only ~40–67% of eroded sand deposited in the depositional lobe. The remaining volumes are deposited downwind, in a larger area, often in vegetated zones as grain fall. Similarly, Zhou et al. (2022) reported that only 30% of sediment from a trough blowout was retained in a depositional lobe over nine years. Arens (2005) showed a loss of ~15% of the eroded volume of a reactivated parabolic dune located in Zuid-Kennemerland. This study shows similar findings for the 2014–2020 period, with a volume loss of the depositional area of approximately 25%. This component is transported farther into the hinterland. In 2020–2023, the Cremermeer parabolic dune maintains a slightly negative balance (~10% sand loss), while both the Houtglop and Wieringen parabolic dunes shift to a positive mass balance. This shift is likely not present in the Cremermeer RPD, since a portion of the eroded sand is transported into the adjacent Cremermeer lake, leading to an apparent underestimation of sediment deposition.

Arens and Van Dijk (2025) also show a change to a positive budget for the Houtglop parabolic dune from −25,918 m^3 (2014–2020) to +1408 m^3 (2020−2022), but the Wieringen parabolic dune remains negative, although the trend of increasing mass balances remains the same, −6358 m^3 (2014–2020) to −1102 m^3 (2020–2022). For the Cremermeer parabolic dune the volumetric change trend is also similar, from −2158 m^3 (2014–2020) to −1804 m^3 (2020–2022). The study also found that there is transport parallel to the dune crest, since the southern sections of both the Houtglop and Wieringen reactivated parabolic dunes have a negative mass balance, while mass balance of the northern parts are positive.

While DEM artifacts (e.g. vegetation) may contribute to apparent mass balance changes, the consistent increase in mass balance of the RPD's suggests a morphodynamic shift. This shift might be a result of an external sediment input. A plausible explanation is the formation of a transport corridor transporting sand from/through the notches into the blowout systems. Petersen et al. (2011) showed suspended sand transport during high wind events reaching parabolic dunes in the hinterland of a vegetated foredune. In this study, the migration of depositional lobes behind the foredune notches may have enhanced this sand transfer into the Houtglop and, subsequently, the Wieringen- and to a lesser extent the Cremermeer parabolic dune systems, explaining the observed positive and less negative mass balances. The alignment of depositional lobes and increased sand capture in downwind sand traps supports this hypothesis. This observation suggests the Noordwest Natuurkern system evolved from a erosional to a possible dynamic depositional landform, achieving one of the goals of the Dutch Dune Revival project.

5.2. *Suspended aeolian sand transport*

The unique sand trap dataset presented in this study confirms that suspended aeolian sand transport extends beyond what is typically visible in geomorphological changes. Suspended sand transport was recorded at all sand traps extending up to 1200 m inland, well beyond

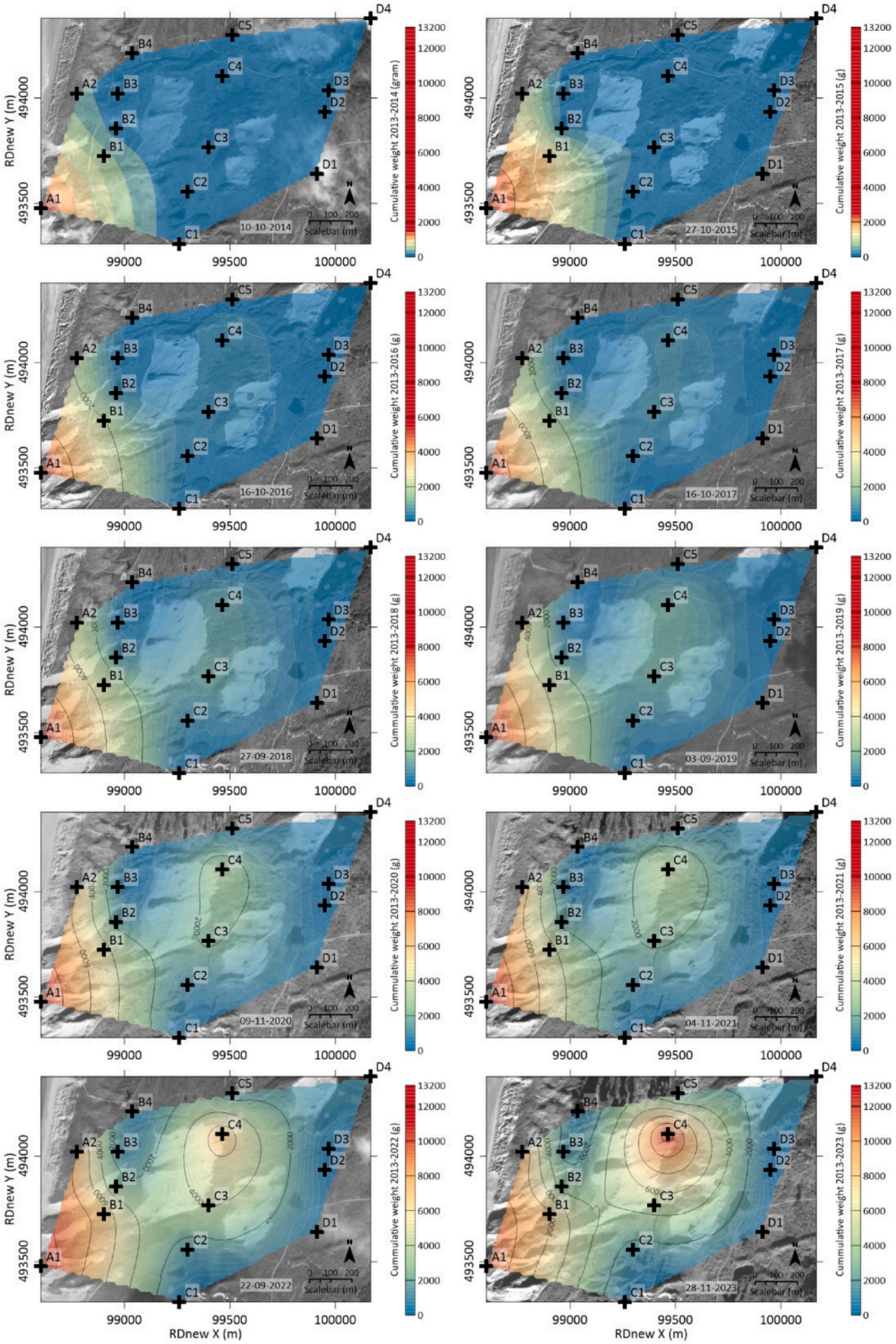


Fig. 9. Cumulative weight of each sand trap between the year 2014 and 2023 plotted as contour maps. The color scale range changes per map based on the maximum cumulative weight value. Each black contour line indicates 2000 g. The contour maps overly the corresponding grayscale satellite image of each year, the date of the image is indicated on each map.

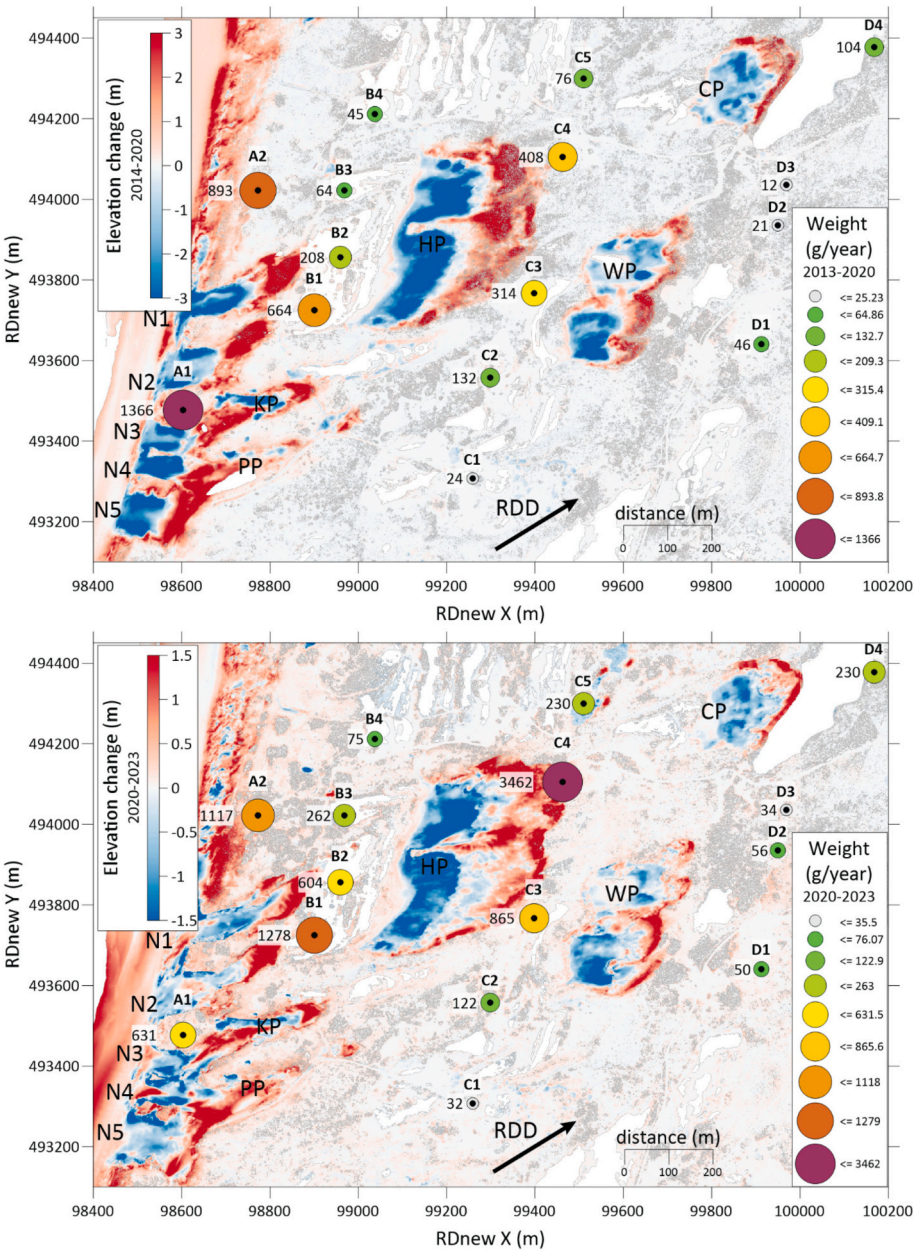


Fig. 10. These maps are similar to Fig. 5, showing positive (red) and negative (blue) surface level changes in two periods on the left 2014–2020 on the right 2020–2023. The average yearly sample weight of each period (2013–2020 and 2020–2023) is plotted as point data with relative size and color. In the first period suspended sand transport is focused at the foredune. In the second period the highest transport occurred behind the Houtglop parabolic dune, showing changes in dynamics between the two periods. The arrow shows the resultant drift direction (RDD) of ~ 59°. The notches are indicated by N1-N5, the Houtglop parabolic by HP, Wieringen parabolic dune (WP) and the Cremermeer parabolic dune (CP).

the zone of visible geomorphological change. This result emphasizes the role of suspension transport as an important but often underestimated part of the sand budget of coastal dune systems.

Previous research (e.g. Arens et al., 2002; Arens et al., 2004; Petersen et al., 2011; Arens et al., 2013b; Bodenbender et al., 2025) indicated the contribution of suspended sediment transport, under strong wind conditions. These studies, however, are largely based on short-term measurements or event scale observations and smaller spatial extents. As a result, these studies provide limited insight in how suspended transport contributes to sediment redistribution at longer temporal and spatial scales. Studying dune systems on longer time scales allows for differentiation between single event responses and morphodynamic behavior. In this study, the temporal suspended load trends validate and extend those findings over a decadal scale, where storm wind conditions (hourly wind speed >20.8 m/s) are a major factor controlling suspended sand transport, while longer-term geomorphological change controls spatial redistribution. Because the impact of storm events on suspended aeolian transport varies strongly between events, multi-year monitoring is required to reliably characterize transport behavior. The results demonstrate that aeolian suspended transport in a remobilized dune is not limited to a zone in the lee of the foredune, but is capable of being transported over larger distances into the hinterland, influencing vegetation, soil development and potential new parabolic dune formation.

In Fig. 10 the average sample weight in g/year is shown per sand trap in relation to the elevation changes. In the period 2014–2020, suspended sand transport is mainly limited to the foredune (A1 and A2) and directly behind the foredune notches (B1). A similar trend was found by Riksen et al. (2016) on Ameland. Sand traps C3 and C4 also show

increased values, related to the Houtglop parabolic dune. Similar to the volumetric calculations, a change occurs in the following period 2020–2023. Here, the highest suspended sand transport is found directly behind the Houtglop parabolic dune, surpassing the foredune transport rates. This relates to the extension of the depositional area of the Houtglop parabolic dune. The source of the suspended sand moves towards the sand traps. This is also evident in sand traps B1 and B2 behind the foredune notches and D2–4 in the hinterland that have (more than) doubled their average yearly sample weight. Sand trap A1 shows a decrease possibly related to bypass of sand transport through the notches. Sand traps such as B1, C1, C2 and D1 do not show a major change. Again this supports the possibility of a transport corridor that has formed between the foredune notches and reactivated parabolic dunes in the hinterland.

5.3. Storm impact

As stated by Ciavola et al. (2015), storms are the most important factor for controlling short-term coastline movement. Storm events are also demonstrably the dominant drivers of suspended sediment transport towards the hinterland of a coastal dune system. These accounted for the highest portion of the total transported sand, although they comprise only a fraction of the time series (up to twelve hours maximum). The total sediment contribution of all storms combined are shown in relation to the geomorphological changes in Fig. 11. At the foredune, sediment contributions of sand traps A1 and A2 are relatively high, these traps are directly influenced by storms. The B-traps show lower contributions, but these traps have not been sampled regularly. In the hinterland, up to 89% of the total suspended sand weight is captured in the C- and D-sand traps during storms. Especially the most distal sand traps (D1–4) are dependent on the storm events, averaging ~80% of the total weight collected. Here, periods of (extended) non-storm wind speeds and wind direction have not been taken into account due to being highly variable. The correlation between storms and spikes in sand trap sample weight suggests that sediment transport models could integrate storm frequency and intensity as primary drivers in long-term morphodynamic models for suspended sand transport, rather than relying primarily on mean wind speeds and average wind vectors.

5.4. Notched- vs unnotched dune system

On decadal timescales, suspended sand transport shows clear contrasts in rates of change between geomorphological settings, rather than being solely controlled by meteorological forcing. Sand traps are grouped into notched and unnotched systems based on their location and differences in the temporal evolution of suspended load (Fig. 12). Traps in the unnotched group (A2, B3, B4, C1, C2, D1) show stable, linear increases in the suspended load curve. In contrast, traps near or downwind of notches and RPD's (A1, B1, B2, C3-C5, D2-D4) show more dynamic patterns. These trends are not driven by wind intensity but rather by trap position relative to landform elements that lie upwind that contribute to long-distance suspension. Sand traps behind foredune notches show a declining trend over time related to decreased transport through the widening notches. In contrast, traps behind RPD's show an increasing trend related to morphological changes created by the downwind migration of sand bodies and the initiation of a possible transport corridor.

5.4.1. Effects of an unnotched foredune: stable suspended load

Traps A2, B3, B4, C1, C2 and D1 possibly reflect baseline conditions before the creation of notches and reactivated parabolic dunes, showing a relatively linear increase in cumulative suspended load over time (Fig. 12). Given their position relative to the resultant drift direction (RDD), these sand traps are not directly influenced by sediment transport associated with foredune notches or RPD's (Fig. 10). A steep drop in suspended sand transport over 200 m inland is observed (Fig. 9), similar to patterns found by Arens et al. (2013b). Elevation data show dune growth near A2, but limited change near the other sand traps (Fig. 10). These stable, linear trends are in line with long-term foredune growth observed along the Dutch coast (De Vries et al., 2012; Ruessink et al., 2022). The unnotched system, represented by sand trap D1, shows no rate of change in between the first five years and the last five years of the dataset (Table 8).

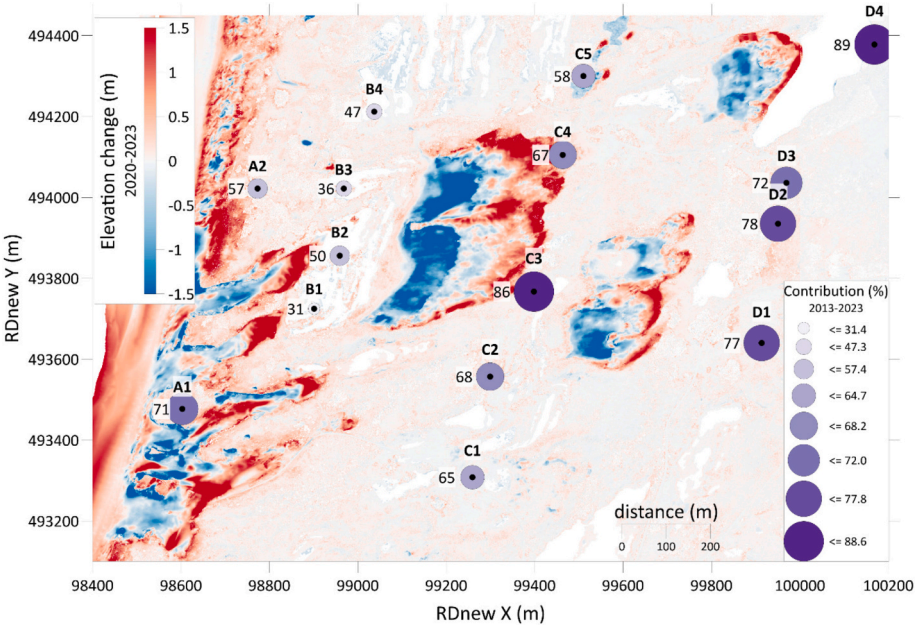


Fig. 11. This map is similar to Fig. 5, showing positive (red) and negative (blue) surface level in the period 2020–2023. The percentual contribution of all storm events between 2013 and 2023 is indicated by point data with relative size and color. These maps show the importance of storm events on suspended transport towards the (distal) hinterland, where percentual values are the highest in the C- and D sand traps. (For interpretation of the references to color in this figure legend, the reader is referred to the web version of this article.)

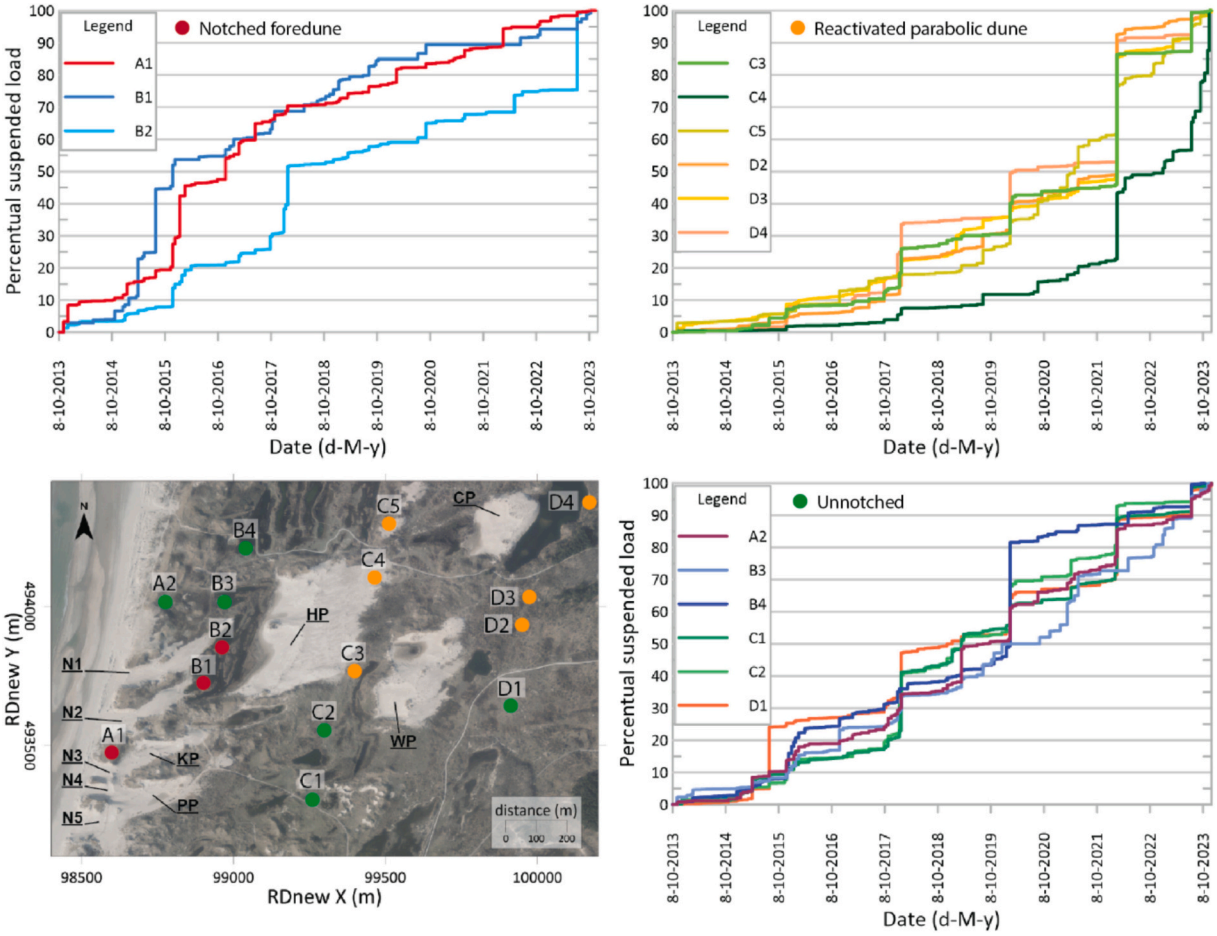


Fig. 12. Subdivision of the cumulative suspended load (%) into the three temporal trend groups. Top left: notched foredune group showing a decreasing trend over time. Top right: reactivated parabolic dune group showing an increasing trend over time. Bottom right: the unnotched group showing a linear trend over time. In the bottom left the sand traps that are represented by the different groups are indicated by a specific color shown in the graphs.

Table 8
Sediment contribution for two equal time intervals, 2013–2018 and 2018–2023 shown as total contribution in percentages per period, and average contribution per year for sand traps A1, C4 and D1. Rates of change are expressed as dimensionless ratios between the contributions of the two multi-year phases and reflect system behavior rather than transport rates. Sand trap A1 is indicative for the notched foredune, sand trap C4 is indicative for the RPD setting and D1 is indicative for the unnotched system.

	Sediment contribution (%)				
Sand trap	2013–2018	2018–2023	Average 2013–2018%/year	Average 2018–2023%/year	Ratio
A1	70.7	29.3	14.1	5.9	0.4
C4	7.5	92.5	1.5	18.5	12.3
D1	49.7	50.3	9.9	10.1	1.0

5.4.2. *Effect of foredune notches: decreasing suspended load*

From 2013 to 2017, notches effectively transported sand inland, aligning with Ruessink et al. (2018). After 2017, a decrease in suspended load, especially in traps A1, B1, and B2 is observed (Fig. 12). This decrease is likely related to widening of the notches, reducing wind acceleration (Van Kuik et al., 2022; Van Westen et al., 2024) and thus the transport capacity of the wind. This results in a smaller suspended load during high wind events. Based on the observed trends the evolutionary stage of the foredune notches in the Kennemerduinen can be characterized as transitioning into a stabilization stage (Talavera et al., 2024; Van Kuik et al., 2022). The ratio between early- and late phase cumulative contributions of sand trap A1 are indicative of the notched system, where in the first 5 years, approximately two-thirds of the total sediment contributions was captured, compared to one-third in the last 5 years (Table 8).

5.4.3. *Effects of reactivated parabolic dunes: increasing suspended load*

Traps downwind of reactivated parabolic dunes (C3–C5, D2–D4) show an increase in cumulative suspended load over time (Fig. 12), indicating active parabolic dune development and the possible formation of a transport corridor. C4, located in the corridor behind the depositional lobe of the Houtglop parabolic dune, recorded the highest total suspended load. Inland D-traps 2–4 also show this trend, with the highest values behind the Cremermeer and Wieringen blowouts. These findings suggest that these blowouts are still in a dynamic, growth/expanding phase (Talavera et al., 2024). A strong rate of change is shown by sand trap C4 where late-phase suspended transport exceeds early-phase values by an order of magnitude (Table 8).

RPD's may function as a depositional sink, but also as secondary sediment source, impacting downwind aeolian sorting trends. Sediment transported through foredune notches has already undergone initial sorting, subsequent remobilization of grains and erosion occurs at the upwind faces of the RPD's, potentially changing aeolian sorting patterns. This implies that RPD's can potentially introduce a stepwise, or repeated sorting pattern of sand grains farther into the hinterland.

5.5. Future research: implications grain fall and ecology

While notches have demonstrated effectiveness based on visible elevation changes (Ruessink et al., 2018; Van Kuik et al., 2022), much of the grain fall in the hinterland is too subtle to be detected by DEM's or remote sensing. As a result, current estimates likely underestimate the total aeolian sand budget, particularly for suspended transport. This study suggests that measurable volumes are transported farther into the hinterland, over distances exceeding 400 m, implying that the ecological and pedological impacts are also likely underestimated.

One of the limitations of this study is the lower sampling resolution of the B-traps. Due to changes in groundwater levels, these traps were periodically surrounded by (deep) water and could not be emptied regularly. This results in a temporal trend bias. Nevertheless, a fixed-location sand trap network, as employed in this study, provides valuable insight into spatial transport patterns of suspended sand. Future research would benefit from real-time, larger scale and higher detail monitoring of sand transport. Instruments such as those described by Pozzebon et al. (2018) could track sand transport along with wind speed, direction, and precipitation, improving alignment between field measurements and aeolian transport models which currently show notable mismatches (Barchyn et al., 2014). A denser grid of sand traps could provide more insight into the area affected by grain fall and improve our understanding of the effects of wind direction on suspension transport in coastal dunes. Since the sand traps used in this study capture sand that is still in transport, it is important to find a correlation with the mass accumulation rate of deposited sand on the surface to complete the full sand budget of a coastal dune system. Developing a sand trap capable of measuring surface accumulation rates would help close the sand budget and quantify grain fall impact.

Additionally, understanding the ecological effects of grain fall requires further investigation into the physical- and mineralogical characteristics of the transported sand. Prior work (Hallin et al., 2019; IJzendoorn et al., 2023) has investigated the critical role of grain size in aeolian transport. Van Hateren et al. (2020) identified three aeolian transport modes from surface samples: bedload, modified saltation, and suspension, based on grain size and shape sorting. Their findings suggest that bedload transport is the main transport mode at the beach and in the notches. Modified saltation transport occurs at the lee-side of the foredune, between the A- and B-traps. Suspension transport dominates in the hinterland zone between the B- and D-traps. A sorting trend is observed where bedload transport consists of large round grains, modified saltation transport is characterized by smaller grainsizes and more elongated large grains. Suspended transport is characterized by the smallest grainsize fraction, together with the most elongated larger grains. Extending these analyses on sand trap samples from this study could help identify areas, based on temporal grain size, grain shape and mineralogy trends, where carbonate and other minerals are enriched by aeolian sorting, which may influence soil development and vegetation succession in the hinterland.

6. Conclusion

This study demonstrates that suspended aeolian sand transport in a remobilized coastal dune system is spatially variable and temporally episodic, with distinct trends in the notched-, unnotched-, and reactivated parabolic dune zones. Storm events, though lasting less than twelve hours, account for the majority of the sediment contribution, up to 89% of the total cumulative weight, emphasizing their dominant role in suspended aeolian sand transport into the hinterland.

The geomorphological evolution of the notches and reactivated parabolic dunes influences the spatial transport patterns. While notches show signs of stabilization, RPD's remain active, even showing an increase in suspended sand transport, suggesting a shift in sediment dynamics by the migration of depositional lobes and the possible formation of a transport corridor. The unnotched dune systems show a continuous trend indicative of the generally linear growth of the Dutch coastal dunes.

During storm events, suspended transport reaches distances of at least 1200 m inland, far beyond the zones of visible geomorphological change. This shows the importance of suspended sand transport in shaping dune morphology, soil development and ecological succession. The areas affected by grain fall behind notches and reactivated parabolic dunes is underrepresented in volumetric calculations and remote sensing studies. The volumetric calculations can be helpful to get better insights into the extent of the depositional areas and volumes that are deposited as grainfall in the hinterland. These findings highlight the need to incorporate suspended aeolian transport into sediment budget calculations and coastal morphodynamic models, especially under changing climate conditions.

This unique dataset contributes as a base to a broader study on aeolian sand transport and sorting processes along the Dutch North Sea coast. Multiple sites in two different coastal districts (carbonate bearing vs. carbonate poor) will be monitored using sand traps. Future work will focus on the characterization of the transported sediment (grain size, grain shape and mineralogy) and quantifying accumulation rates of deposited suspended sand, to better understand sorting patterns, soil development and ecological impacts. Integrating real-time monitoring of transport and meteorological conditions could also improve model calibration and forecasting of aeolian transport.

CRediT authorship contribution statement

O. Verhage: Writing – original draft, Visualization, Methodology, Investigation, Formal analysis, Data curation, Conceptualization. **S.M. Arens:** Writing – review & editing, Visualization, Resources, Methodology, Investigation, Data curation, Conceptualization. **C.J. Beets:** Writing – review & editing, Supervision, Methodology, Conceptualization. **J.B.W. Stuut:** Writing – review & editing, Supervision, Methodology, Conceptualization. **G. van Zijl:** Resources, Methodology, Data curation. **M.A. Prins:** Writing – review & editing, Supervision, Methodology, Conceptualization.

Declaration of competing interest

The authors declare the following financial interests/personal relationships which may be considered as potential competing interests: Oeki Verhage reports financial support was provided by VU Amsterdam. Oeki Verhage reports a relationship with VU Amsterdam that includes: employment. If there are other authors, they declare that they have no known competing financial interests or personal relationships that could have appeared to influence the work reported in this paper.

Acknowledgements

The authors would like to express their sincere gratitude to all those who contributed to this research for their valuable insights and discussion throughout the course of this study. We also thank the two anonymous reviewers and the associate editor of *Aeolian Research* for their positive and constructive feedback, which significantly improved the manuscript. For his dedication to the project, we like to thank Gerard van Zijl for sampling and maintaining the sand traps, and drying and weighing all collected samples over the past decade. We also thank PWN for the support and their provision of essential facilities and access to the research area, in particular we like to acknowledge Marieke Kuipers.

The Noordwest Natuurkern is part of the Dutch Dune Revival project (LIFE09 NAT/NL/000418) funded by the European LIFE+ Nature fund, the Provincie Noord-Holland, PWN and Natuurmonumenten.

Appendix A. Supplementary data

Supplementary data to this article can be found online at https://doi.

org/10.1016/j.aeolia.2026.101063.

Data availability

Data will be made available on request.

References

Aggenbach, C., Arens, S., Fujita, Y., Kooijman, A., Neijmeijer, T., Nijssen, M., Stuyfzand, P., van Til, M., van Boxel, J., & Cammeraat, L. (2018). Herstel grijze duinen door reactiveren kleinschalige dynamiek (OBN223-DK). VBNE, Driebergen. UvA-DARE 63879529.

Anderson, J.L., Walker, I.J., 2006. Airflow and sand transport variations within a backshore–parabolic dune plain complex: NE Graham Island, British Columbia, Canada. Geomorphology 77 (1–2), 17–34. https://doi.org/10.1016/j.geomorph.2005.12.008.

Arens, S.M., 1996. Patterns of sand transport on vegetated foredunes. Geomorphology 17 (4), 339–350. https://doi.org/10.1016/0169-555X(96)00016-5.

Arens, S.M., 2005. Reactivatie van de Bruid van Haarlem situatie 2005 (RAP2005.05). Arens Bureau voor Strand- en Duinonderzoek. , commissioned by. PWN Waterleidingbedrijf Noord-Holland. https://www.duinonderzoek.nl/wp-content/uploads/2016/07/bruid_2005.

Arens, S.M., van Dijk, P., 2025. *Noordwest Natuurkern: Effecten van ingrepen op dynamiek – Resultaten monitoring 2022–2024* (RAP2025.02). Arens Bureau voor Strand- en Duinonderzoek. , commissioned by. PWN Waterleidingbedrijf Noord-Holland.

Arens, S.M., Wiersma, J., 1994. The Dutch foredunes: inventory and classification. J. Coast. Res. 10 (1), 189–202 (Fort Lauderdale (Florida), ISSN 0749-0208).

Arens, S.M., van Kaam-Peters, H.M.E., van Boxel, J.H., 1995. Air flow over foredunes and implications for sand transport. Earth Surf. Process. Landf. 20 (4), 315–332. https://doi.org/10.1002/esp.3290200403.

Arens, S.M., van Boxel, J.H., Abuodha, J.O.Z., 2002. Changes in grain size of sand in transport over a foredune. Earth Surf. Process. Landf. 27 (11), 1163–1175. https://doi.org/10.1002/esp.418.

Arens, S.M., Slings, Q.L., de Vries, C.N., 2004. Mobility of a remobilised parabolic dune in Kennemerland, The Netherlands. Geomorphology 59 (1–4), 175–188. https://doi.org/10.1016/j.geomorph.2003.09.014.

Arens, S.M., Everts, F., Kooijman, A., Leek, S., Nijssen, M., & de Vries, N. (2012). Ecologische effecten van zandsuppletie op de duinen langs de Nederlandse kust. Rapport Bosschap OBN166-DK, Directie Kennis en Innovatie, Ministerie van ELI en Rijkswaterstaat Waterdienst.

Arens, S.M., Mulder, J.P.M., Slings, Q.L., Geelen, L.H.W.T., Damsma, P., 2013a. Dynamic dune management, integrating objectives of nature development and coastal safety: examples from the Netherlands. Geomorphology 199, 205–213. https://doi.org/10.1016/j.geomorph.2012.10.034.

Arens, S.M., Everts, F.H., Kooijman, A.M., Lammerts, E.J., Leek, S.T., Nijssen, M.E., van der Valk, B., de Vries, N.P.J., 2013b. Geomorfologische en ecologische effecten van zandsuppleties op duinen. De Levende Natuur 114 (6), 246–251 (No DOI available; open access at Natuurtijdschriften-pub-580514).

Arens, S. M., et al. (2020). Comment on 'is 're-mobilisation' nature restoration or nature destruction? A commentary' by I. Delgado-Fernandez, R.G.D. Davidson-Arnott & P. A. Hesp. *J. Coast. Conserv., 24*, article 17. doi:https://doi.org/10.1007/s11852-020-00731-1.

Bagnold, R. (1941). The effect of sand movement on the surface wind. In The Physics of Blown Sand and Desert Dunes (pp. 57–76). Springer. (Reprinted by Dover Publications (2005). ISBN: 9780486439310).

Baird, T.R., Bristow, C.S., Luo, W., Du, E., Bryant, R.G., Mitchell, T.M., Vermeesch, P., 2021. Blowout morphometrics and mass balances. Front. Earth Sci. 9, 669440. https://doi.org/10.3389/feart.2021.669440.

Bakker, T. W. M. (1981). Nederlandse kustduinen: geohydrologie. Wageningen: Pudoc. ISBN: 90–220–0758-8.

Barchyn, T.E., Martin, R.L., Kok, J.F., Hugenholtz, C.H., 2014. Fundamental mismatches between measurements and models in aeolian sediment transport prediction: the role of small-scale variability. Aeolian Research 15, 245–251. https://doi.org/10.1016/j.aeolia.2014.07.002.

Bird, T.L.F., Bouskila, A., Groner, E., Bar Kutiel, P., 2020. Can vegetation removal successfully restore coastal dune biodiversity? Appl. Sci. 10 (7), 2310. https://doi.org/10.3390/app10072310.

Bodenbender, B., Yurk, B., DeVries-Zimmerman, S., Harlow, B., Schaetzl, R.J., Hansen, E., 2025. Suspended sediment transport over the lee slope and forest canopy downwind of a large blowout/parabolic dune. Aeolian Res. 73, 100974. https://doi.org/10.1016/j.aeolia.2025.100974.

Brand, E., Ramaekers, G., Lodder, Q., 2022. Dutch experience with sand nourishments for dynamic coastline conservation – an operational overview. Ocean Coastal Manage. 217, 106008. https://doi.org/10.1016/j.ocecoaman.2021.106008.

Ciavola, P., Ferreira, Ó., van Dongeren, A., van Thiel de Vries, J., Armaroli, C., Harley, M., 2015. Prediction of storm impacts on beach and dune systems. In: Quevauviller, P. (Ed.), Hydrometeorological Hazards: Interfacing Science and Policy. Wiley, pp. 219–244. https://doi.org/10.1002/9781118629567.ch3d.

Cooper, A., Jackson, D., 2021. A global 'greening' of coastal dunes: an integrated consequence of climate change? Glob. Planet. Change 53 (2), 345–352. https://doi.org/10.1016/j.gloplacha.2019.103026.

Creer, J., Litt, E., Ratcliffe, J., Rees, S., Thomas, N., & Smith, P. (2020). A comment on some of the conclusions made by Delgado-Fernandez et al. (2019). "Is 're-mobilisation' nature conservation or nature destruction? A commentary".. J. Coast. Conserv., 24, Article 29. doi:https://doi.org/10.1007/s11852-020-00745-9.

De Jong, B., Keijsers, J.G.S., Riksen, M.J.P.M., Krol, J., Slim, P.A., 2014. Soft engineering vs. a dynamic approach in coastal dune management: A case study on the North Sea barrier island of Ameland, the Netherlands. J. Coast. Res. 30 (4), 670–684. https://doi.org/10.2112/JCOASTRES-D-13-00125.1.

De Ruig, J., 1989. De sedimentbalans van de gesloten Hollandse kust over de periode 1963 tot 1986. Rijkswaterstaat. . GWAO-89.016 ZL-NXL89. 42. TU Delft Repository.

De Vries, S., Southgate, H.N., Kanning, W., Ranasinghe, R., 2012. In: Kranenburg, W.M., Horstman, E.M., Wijnberg, K.M. (Eds.), Dune development and aeolian transport along the Holland coast. University of Twente, pp. 41–53. https://doi.org/10.3990/2.182. Jubilee Conference Proceedings NCK-Days 2012: Crossing Borders in Coastal Research.

Delgado-Fernandez, I., Davidson-Arnott, R.G., Hesp, P.A., 2019. Is 're-mobilisation'nature restoration or nature destruction? A commentary. J. Coast. Conserv. 23 (6), 1093–1103. https://doi.org/10.1007/s11852-019-00716-9.

Eisma, D., 1968. Composition, origin and distribution of Dutch coastal sands between Hoek van Holland and the island of Vlieland. Neth. J. Sea Res. 4 (2), 123–267. https://doi.org/10.1016/0077-7579(68)90011-2.

Fryberger, S.G., Dean, G., McKee, E.D., 1979. Dune forms and wind regime. In: A study of global sand seas, 1052. Geological Survey (US), pp. 137–170.

Gibbard, P.L., 1988. The history of the great northwest European rivers during the past three million years. Philos. Trans. R. Soc., B 318 (1191), 559–602. https://doi.org/10.1098/rstb.1988.0024.

Hallin, C., Larson, M., Hanson, H., 2019. Simulating beach and dune evolution at decadal to centennial scale under rising sea levels. PloS One 14 (4), e0215651. https://doi.org/10.1371/journal.pone.0215651.

Hesp, P.A., 2002. Foredunes and blowouts: initiation, geomorphology and dynamics. Geomorphology 48 (1–3), 245–268. https://doi.org/10.1016/S0169-555X(02)00184-8.

Hesp, P.A., Smyth, T.A.G., 2016. Jet flow over foredunes. Earth Surf. Process. Landf. 41 (12), 1727–1735. https://doi.org/10.1002/esp.3945.

Hesp, P.A., Walker, I.J., Chapman, C., Davidson-Arnott, R., Bauer, B.O., 2013. Aeolian dynamics over a coastal foredune, Prince Edward Island, Canada. Earth Surf. Process. Landf. 38 (13), 1566–1575. https://doi.org/10.1002/esp.3444.

Hugenholtz, C.H., Wolfe, S.A., 2006. Morphodynamics and climate controls of two aeolian blowouts on the northern Great Plains, Canada. Earth Surface Processes and Landforms: the Journal of the British Geomorphological Research Group 31 (12), 1540–1557. https://doi.org/10.1002/esp.1367.

Hugenholtz, C.H., Wolfe, S.A., Walker, I.J., Moorman, B.J., 2009. Spatial and temporal patterns of aeolian sediment transport on an inland parabolic dune, Bigstick Sand Hills, Saskatchewan, Canada. Geomorphology 105 (1–2), 158–170. https://doi.org/10.1016/j.geomorph.2007.12.017.

Jelgersma, S., de Jong, J., Zagwijn, W.H., van Regteren Altena, J.F., 1970. The coastal dunes of the western Netherlands: geology, vegetational history and archeology. Med. Rijks Geol. Dienst. 21, 93–167.

Klijn, J.A., 1981. *Nederlandse kustduinen: geomorfologie en bodems* [Doctoral thesis, Wageningen University]. Centrum voor Landbouwpublikaties en Landbouwdocumentatie. https://doi.org/10.18174/206778.

Kooijman, A.M., 2004. Environmental problems and restoration measures in coastal dunes in the Netherlands. In: Martínez, M.L., Psuty, N.P. (Eds.), Coastal Dunes: Ecology and Conservation. Springer, pp. 243–258. https://doi.org/10.1007/978-3-540-74002-5_15.

Kooijman, A.M., de Haan, M.W.A., 1995. Grazing as a measure against grass encroachment in Dutch dry dune grassland: effects on vegetation and soil. J. Coast. Conserv. 1, 127–134. https://doi.org/10.1007/BF02905121.

Kuipers, M., Van der Vegte, J., 2016. Layman's report: Dutch Dune Revival in Zuid-Kennemerland: de Noordwest Natuurkern en Levend Duin. Natuurmonumenten. PWN. . LIFE+ Nature Project LIFE09NAT/NL/000418.

Kuipers, M., Arens, S. M., & Ruessink, B. G. (2016). Grootschalig herstel van stuivende duinen. *Lev. Nat., 117*(3), 90–93. Natuurtijdschriften-pub-718337.

Lansu, E.M., Reijers, V.C., Höfer, S., Luijendijk, A., Rietkerk, M., Wassen, M.J., Lammerts, E.J., van der Heide, T., 2024. A global analysis of how human infrastructure squeezes sandy coasts. Nat. Commun. 15 (1), 432. https://doi.org/10.1038/s41467-023-44659-0.

Leatherman, S.P., 1978. A new aeolian sand trap design. Sedimentology 25 (2), 303–306. https://doi.org/10.1111/j.1365-3091.1978.tb00315.x.

Meerkerk, A., Arens, S.M., van Lammeren, R.J.A., Stuiver, H.J., 2007. Sand transport dynamics after a foredune breach: A case study from Schoorl, the Netherlands. Geomorphology 86 (1–2), 52–60. https://doi.org/10.1016/j.geomorph.2006.08.007.

Miyanishi, K., Johnson, E.A., 2021. Coastal dune succession and the reality of dune processes. In: Johnson, E.A., Miyanishi, K. (Eds.), Plant Disturbance Ecology: The Process and the Response, 2nd ed. Academic Press, pp. 253–290. https://doi.org/10.1016/B978-0-12-818813-2.00007-1.

Nawarat, K., Reyns, J., Vousdoukas, M. I., Duong, T. M., Kras, E., & Ranasinghe, R. (2024). Coastal hardening and what it means for the world's sandy beaches. *Nat. Commun.,* 15(1), Article 54952. doi:https://doi.org/10.1038/s41467-024-54952-1.

Nguyen, D., Hilton, M., Wakes, S., Simons-Smith, T., 2021. Incident wind angle and topographic steering through excavated foredune notches. Geomorphology 395, 107982. https://doi.org/10.1016/j.geomorph.2021.107982.

Nguyen, D., Hilton, M., Wakes, S., 2022. Wind flow dynamics and sand deposition behind excavated foredune notches on developed coasts. Earth Surf. Process. Landf. 47 (7), 1698–1719. https://doi.org/10.1002/esp.5341.

Nickling, W.G., Davidson-Arnott, R.G.D., 1990. Aeolian sediment transport on beaches and coastal sand dunes. Proceedings of the Canadian Symposium on Coastal Sand Dunes. . (Publication/274192369).

Noest, V., van der Maarel, E., van der Meulen, F., 1995. Impact of climatic change on the ecology of temperate coastal wetlands, beaches, and dunes. In: Eisma, D. (Ed.), Climate Change: Impact on Coastal Habitation. CRC Press, pp. 189–207. https://doi.org/10.1201/9781003069935-9.

Pagon, T., Smyth, T., Wilson, R., Fox, B., 2025. Distribution and constructed morphology of artificial foredune notches. Earth Surf. Process. Landf. 50 (7), e70094. https://doi.org/10.1002/esp.70094.

Pearce, K.I., Walker, I.J., 2005. Frequency and magnitude biases in the 'Fryberger' model, with implications for characterizing geomorphically effective winds. Geomorphology 68 (1–2), 39–55. https://doi.org/10.1016/j.geomorph.2004.09.030.

Petersen, P.S., Hilton, M.J., Wakes, S.J., 2011. Evidence of aeolian sediment transport across an *Ammophila arenaria*-dominated foredune, Mason Bay, Stewart Island. N. Z. Geogr. 67 (3), 174–189. https://doi.org/10.1111/j.1745-7939.2011.01210.x.

Pozzebon, A., Cappelli, I., Mecocci, A., Bertoni, D., Sarti, G., Alquini, F., 2018. A wireless sensor network for the real-time remote measurement of aeolian sand transport on sandy beaches and dunes. Sensors 18 (3), 820. https://doi.org/10.3390/s18030820.

Riksen, M.J.P.M., Goossens, D., Huiskes, H.P.J., Krol, J., Slim, P.A., 2016. Constructing notches in foredunes: effect on sediment dynamics in the dune hinterland. Geomorphology 253, 340–352. https://doi.org/10.1016/j.geomorph.2015.10.021.

Robin, N., Billy, J., Nicolae Lerma, A., Castelle, B., Hesp, P.A., Rosebery, D., Fauny, C., Deparis, J., Marieu, V., Bouchet, C., 2023. Natural remobilization and historical evolution of a modern coastal transgressive dune field. Earth Surf. Process. Landf. 48 (5), 1064–1083. https://doi.org/10.1002/esp.5535.

Ruessink, B.G., Arens, S.M., Kuipers, M., Donker, J.J.A., 2018. Coastal dune dynamics in response to excavated foredune notches. Aeolian Research 31, 3–17. https://doi.org/10.1016/j.aeolia.2017.07.002.

Ruessink, G., Groenendijk, D., & Arens, S. M. (2024). Digital elevation models and Orthomosaics of the Dutch Noordwest Natuurkern foredune restoration project. Data, *9*(2), Article 37. doi:https://doi.org/10.3390/data9020037.

Ruessink, G., Regtien, J., Gargari, S.F., Arens, B., 2026. Aeolian activity in foredune notches: evidence from multiannual wind observations. Geomorphica 2 (2). https://doi.org/10.59236/geomorphica.v2i2.67.

Schendelaar, J. K. (1984). Enkele opmerkingen over het verband tussen het Rijngedeelte van het Fluviatiele district en het Duindistrict. *Gorteria, 12*(3), 43–50. Repository Naturalis Biodiversity Center pub526768.

Ruessink, G., Sterk, G., Smit, Y., De Winter, W., Hage, P., Donker, J.J., Arens, S.M., 2022. Predicting monthly to multi-annual foredune growth at a narrow beach. Earth Surface Processes and Landforms 47 (7), 1845–1859. https://doi.org/10.1002/esp.5350.

Stuyfzand, P.J., Arens, S.M., Oost, A.P., 2010. Geochemische effecten van zandsuppleties langs Hollands kust. . Bosschap, Rapport nr. 2010/OBN141-DK.. https://vliz.be/imisdocs/publications/ocrd/224373.

Talavera, L., Costas, S., Ferreira, Ó., 2024. Controls on blowout evolution in southern Portugal: A 49-year analysis. Sci. Total Environ. 905, 176769. https://doi.org/10.1016/j.scitotenv.2024.176769.

TNO-GDN, 2025. Schoorl Member. . *In: Stratigraphic Nomenclature of the Netherlands, TNO – Geological Survey of the Netherlands.* Accessed on 02-10-2025 from. https://www.dinoloket.nl/en/stratigraphic-nomenclature/schoorl-member.

Van der Meulen, F., Jungerius, P.D., 1989. Landscape development in Dutch coastal dunes: the breakdown and restoration of geomorphological and geohydrological processes. Proceedings of the Royal Society of Edinburgh, Section B: Biological Sciences 96, 219–229. https://doi.org/10.1017/S0269727000010940.

Van Hateren, J.A., van Buuren, U., Arens, S.M., van Balen, R.T., Prins, M.A., 2020. Identifying sediment transport mechanisms from grain size–shape distributions, applied to aeolian sediments. Earth Surf. Dyn. 8 (2), 527–553. https://doi.org/10.5194/esurf-8-527-2020.

Van IJzendoorn, C.O., Hallin, C., Reniers, A.J.H.M., de Vries, S., 2023. Modeling multi-fraction coastal aeolian sediment transport with horizontal and vertical grain-size variability. J. Geophys. Res. Earth Surf. 128 (7), e2023JF007155. https://doi.org/10.1029/2023JF007155.

Van Kuik, N., de Vries, J., Schwarz, C., Ruessink, G., 2022. Surface-area development of foredune trough blowouts and associated parabolic dunes quantified from time series of satellite imagery. Aeolian Res. 57, 100812. https://doi.org/10.1016/j.aeolia.2022.100812.

Van Soest, J.L., 1929. Plantengeografische districten in Nederland. De levende natuur 33 (10), 311–318.

Van Straaten, L.M.J.U., 1961. Directional effects of winds, waves and currents along the Dutch North Sea coast. Geol. Mijnb. 40, 333–346. https://www.vliz.be/imisdocs/publications/56624.

Van Westen, B., de Vries, S., Cohn, N., van IJzendoorn, C., Strypsteen, G., Hallin, C., 2024. AeoLiS: numerical modelling of coastal dunes and aeolian landform development for real-world applications. Environ. Model. Softw. 179, 106093. https://doi.org/10.1016/j.envsoft.2024.106093.

Walker, I.J., 1999. Secondary airflow and sediment transport in the lee of a reversing dune. Earth Surf. Process. Landf. 24 (5), 437–448. https://doi.org/10.1002/(SICI)1096-9837(199905)24:5<437::AID-ESP999>3.0.CO;2-Z.

Walker, I.J., Hesp, P.A., 2013. Fundamentals of aeolian sediment transport: Airflow over dunes. In: Shroder, J. (Ed.), Treatise on Geomorphology, Volume 11: Aeolian Geomorphology. Academic Press, pp. 109–133. https://doi.org/10.1016/B978-0-12-374739-6.00300-6.

Zhou, Y., Hasi, E., Wang, Z., Qing, D., Han, X., Yin, J., Wu, Z., 2022. Dynamics of blowouts indicating the process of grassland desertification. Land Degrad. Dev. 33 (15), 2885–2897. https://doi.org/10.1002/ldr.4362.